Numerical model investigations on coastal structures with shallow foreshores

Validation of numerical models based on physical model tests on the Petten Sea-defence

May 2000

WL | delft hydraulics

Numerical model investigations on coastal structures with shallow foreshores

Validation of numerical models based on physical model tests on the
Petten Sea-defence
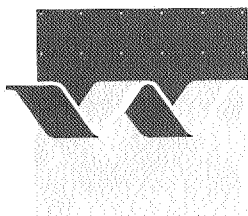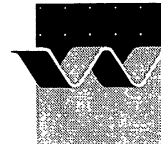
M.R.A. van Gent and N. Doorn

May 2000

WL | delft hydraulics

WL | delft hydraulics

CLIENTS:	Commission of the European Communities; MAST-OPTICREST (MAS3-CT97-0116), Rijkswaterstaat, Dienst Weg- en Waterbouwkunde, WL	DELFT HYDRAULICS

TITLE:	Numerical model investigations on coastal structures with shallow foreshores; Validation of numerical models based on physical model tests on the Petten Sea-defence

ABSTRACT: Within the framework of the European MAST-OPTICREST project prototype measurements, physical model investigations and numerical model investigations have been performed. This report describes comparisons between the test results of two-dimensional physical model investigations on the Petten Sea-defence ("Pettemer Zeewering") and numerical model computations.

Two numerical models have been applied to model wave propagation over the shallow foreshore and one numerical model has been applied to model wave motion on the structure. The models applied for wave propagation over the shallow foreshore are a spectral wave model (SWAN) and a time-domain model (a preliminary version of the Boussinesq-type model TRITON). The model applied for modelling wave motion on the structure is a time-domain model based on the non-linear shallow-water wave equations (ODIFLOCS).

The complex shallow foreshore affects the waves considerably before they reach the toe of the dike. The severe wave breaking and surfbeat phenomena cause that wave propagation over the shallow foreshore is extremely complex, which is also the case for the wave motion on the complex structure. Therefore, this situation is considered as difficult to accurately model numerically. However, valuable predictions can already be obtained from the present versions of the models.

REV.	ORIGINATOR		DATE	REMARKS	REVIEW		APPROVED BY	
0	M.R.A. van Gent		Dec. 1999	Preliminary	N. Doorn		W.M.K. Tilmans	
1	Van Gent/Doorn		April 2000	Draft	M.J.A. Borsboom		W.M.K. Tilmans	
2	Van Gent/Doorn		May 2000	Final	M.J.A. Borsboom		W.M.K. Tilmans	

KEYWORDS	STATUS
Numerical modelling Physical model tests Shallow foreshores Wave run-up Dikes	☐ PRELIMINARY ☐ DRAFT ☒ FINAL

PROJECT IDENTIFICATION: H3129/H3351

Contents

List of Tables

List of Figures

List of Symbols

Acknowledgements

References

Tables

Figures

List of Tables

In text:

In Appendix Tables:

List of Figures

In text:

In Appendix Figures:

List of Symbols

Roman letters:

a	:	friction coefficient for laminar contribution of porous flow (s/m)
b	:	friction coefficient for turbulent contribution of porous flow (s^2/m^2)
c_A	:	coefficient for added mass (-)
c_g	:	group velocity (m/s)
d	:	water depth during still-water (m)
E	:	energy density (m^2/Hz)
f	:	friction coefficient (-)
f_p	:	scaling parameter for wave breaking in Boussinesq-type model (-)
g	:	gravitational acceleration (m/s^2)
H	:	wave height, for regular/monochromatic waves (m)
$H_{1/3}$	:	significant wave height; mean of the highest one-third of the waves (m)
H_{m0}	:	spectral 'significant wave height', $H_{m0} = 4\sqrt{m_0}$ (m)
H_s	:	significant wave height; mean of the highest one-third of the waves: $H_{1/3}$ (m)
h	:	water depth or total thickness of waterlayer (m)
k	:	wave number (-)
m_n	:	n^{th} moment of the frequency spectrum.
m_0	:	variance of the water surface elevation, *i.e.* the total wave energy (m^2)
N	:	wave action density (m^2/Hz^2)
n	:	porosity (-)
q	:	flow from permeable region to free surface region (m/s)
S	:	source terms in spectral wave action balance (m^2)
s	:	wave steepness, for regular/monochromatic waves, $s=2\pi/g \cdot H/T^2$ (-)
s_{-1}	:	wave steepness based on a spectral wave period, $s_{-1}=2\pi/g \cdot H_s/T_{m-1,0}^2$ (-)
T	:	wave period, for regular/monochromatic waves (s)
$T_{m-1,0}$	:	wave period based on $zero^{th}$ and first negative spectral moment (s)
T_p	:	peak wave period, defined as the wave period in an arbitrary wave energy spectrum where the spectral density has a global maximum (s)
$t_{1/2}$	:	measure related to the time required for the wave to pass through the breaking process (s)
u	:	velocity (m/s)
$z_{N\%}$	:	wave run-up level relative to the still-water level, unless denoted relative to NAP, exceeded by $N\%$ of the incident waves (m)

Greek letters:

δ	:	roller thickness in Boussinesq-type model (m)
γ	:	total reduction factor for wave run-up (-)
φ	:	slope of structure (°)

v_t	:	turbulence viscosity (m^2/s)
θ	:	wave direction (°)
σ	:	relative frequency (moving with current) (Hz)
$\xi_{s,-1}$	:	surf-similarity parameter at toe of structure, $\xi_{s,-1}$=tan $\varphi/\sqrt{s_{-1}}$ (-)
ϕ_{ini}	:	angle of the surface for initiation of wave breaking (°)
ϕ_{ter}	:	angle of the surface for which wave breaking is terminated (°)

Abbreviations:

NAP	:	Dutch vertical reference level.
SWL	:	Still Water Level, relative to NAP (m)

1   Introduction

1.1   General

Within the Dutch research framework 'Wave propagation over shallow foreshores' attention is given to the effects of shallow foreshores on wave run-up and wave overtopping. The present numerical model investigations contribute to this research topic. Within the framework of the European MAST-OPTICREST project prototype measurements and physical model investigations are performed on the Petten Sea-defence ('Pettemer Zeewering'). This dike is of special interest since the complex shallow foreshore affects the waves considerably before they reach the toe of the dike. The effects of such shallow foreshores on wave run-up are not sufficiently known. To increase knowledge on these effects not only prototype and laboratory measurements are performed but also numerical model investigations may contribute. Therefore, numerical models are validated using this data-set on the Petten Sea-defence. The present report describes numerical model investigations on the Petten Sea-defence using two numerical models for modelling wave propagation over shallow foreshores and two numerical models for modelling the wave motion on the dike itself.

To predict wave run-up and wave overtopping in other situations than the measured conditions for the Petten Sea-defence, the results need to become available in a more generic way such as in predictive models and design formulae. This report provides insight in the possibilities of available predictive models to model numerically the very complex phenomena involved in wave propagation over shallow foreshores and the resulting wave motion on coastal structures. None of the applied numerical models is developed to such a stage that all relevant phenomena are incorporated in the models. Therefore, these investigations should be considered as investigations which also provide insight in to which extent applied assumptions and phenomena that are not incorporated, prevent accurate modelling of the processes involved with shallow foreshores. This provides valuable insight for further development of the numerical models.

The numerical models are applied on the foreshore and the dike of the Petten Sea-Defence, assuming a situation with no variation in the direction parallel to the coastline; two-dimensional model tests on the Petten Sea-defence are used for comparison (Van Gent, 1999-b). The numerical models applied are one-dimensional versions of a spectral wave model and a time-domain model for the wave propagation over the foreshore (SWAN and the Boussinesq-type model TRITON respectively) and a time-domain model for the wave motion on the dike (ODIFLOCS). Valuable insight would also have been obtained if the model SURFBEAT (Roelvink, 1993), which models the propagation of wave groups and their associated long wave motion, would have been applied but this was beyond the anticipated efforts of these investigations.

Related studies performed within the above mentioned framework are described in Groenendijk (1998), Groenendijk and Van Gent (1998) and Battjes and Groenendijk (1999) as far as wave height statistics on shallow foreshores are concerned, in Van Gent (1999-a) as far as numerical model investigations on wave run-up and wave overtopping for situations with shallow foreshores are concerned and in Van Gent (1999-b) as far as physical model investigations on the Petten Sea-defence are concerned.

The studies described in this report were performed under supervision of dr. M.R.A. van Gent with also contributions by ms. S.C. Beck as visiting researcher from Leichtweiss Institut für Wasserbau (Chapter 4) and dr. M.J.A. Borsboom, ms. N. Doorn, dr. J. Groeneweg (Chapter 3), dr. R.C. Ris and ms. C.M.G. Somers (Chapter 2) from WL | DELFT HYDRAULICS.

1.2   Purpose of numerical model investigations

The purpose of these numerical model investigations is to study to which extent available numerical models are capable of modelling wave propagation over shallow foreshores and the resulting wave motion on dikes. As practical test-case the situation of the Petten Sea-defence is used. This situation with a complex shallow foreshore with wave breaking on two bars, generating also a large amount of energy in long waves, and also a dike with a complex shape and a toe in shallow water, can be regarded as one of the most difficult practical applications for numerical wave models.

1.3   Description of physical model tests

The physical model tests performed for studying the Petten Sea-defence were performed in a wave flume where about 1 km of the foreshore was schematised. Seaward of this part of the foreshore an offshore bar is present on which wave breaking occurs under storm conditions ('Pettemer Polder'). For those tests in the physical model investigations that were aimed at representing measured storm conditions the effects of this bar were accounted for by generating the wave energy spectra that were measured (far) behind this bar in prototype. A second bar, closer to the dike, was modelled in the flume. Figure 1.1 shows the foreshore as constructed in the flume. This figure also shows at which locations wave conditions were measured during the tests. Figure 1.2 shows the dike as modelled in the flume.

Conditions that occurred in 6 storm periods for which prototype measurements were available were studied. Also conditions to study the influence of several parameters such as wave height, wave steepness, spectral shape, water level were studied. In addition, tests with regular waves were performed for validation of numerical models, especially for analysis of surface elevations on the slope.

Figure 1.1 Model set-up in physical model tests (foreshore).
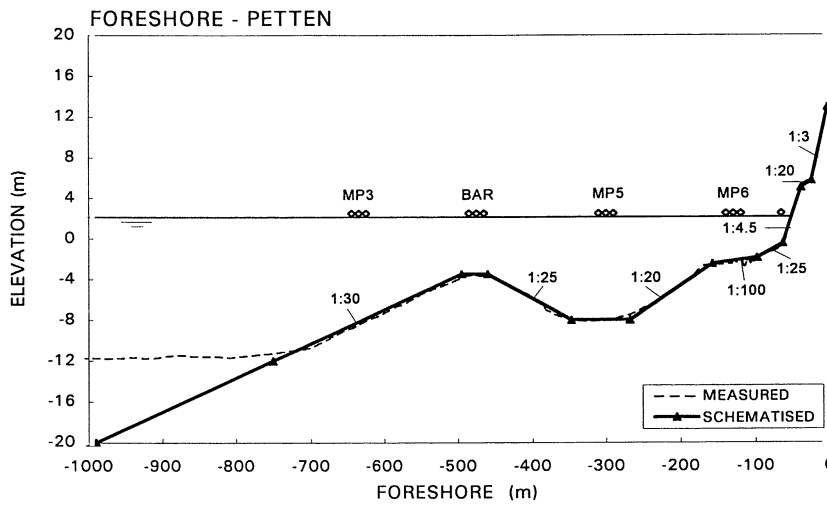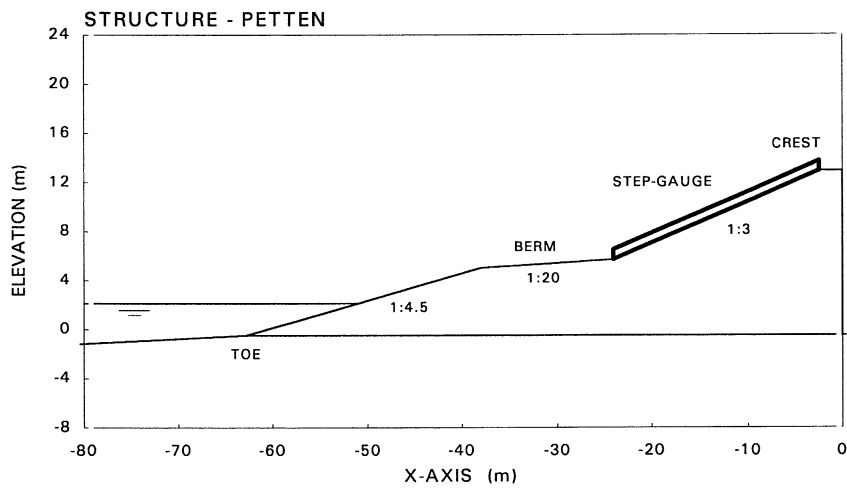

Figure 1.2 Model set-up in physical model tests (dike).
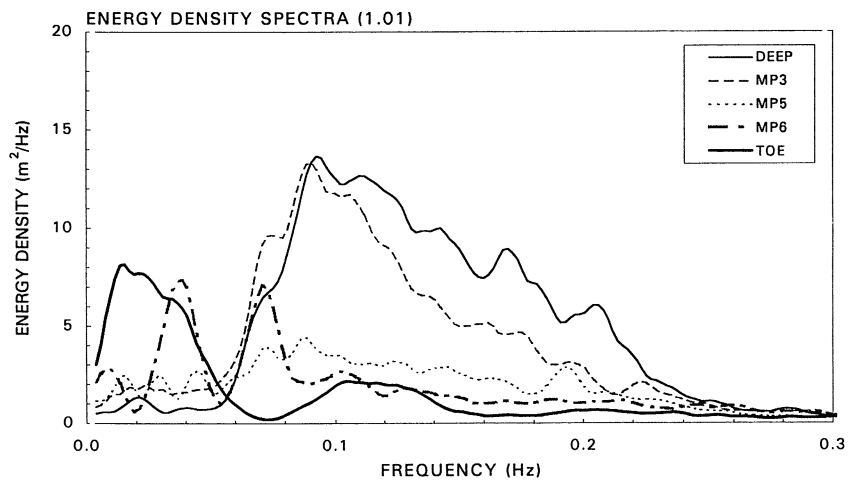
Figure 1.3 Measured wave energy spectra at several locations on the foreshore.

WAVE HEIGHTS ON FORESHORE
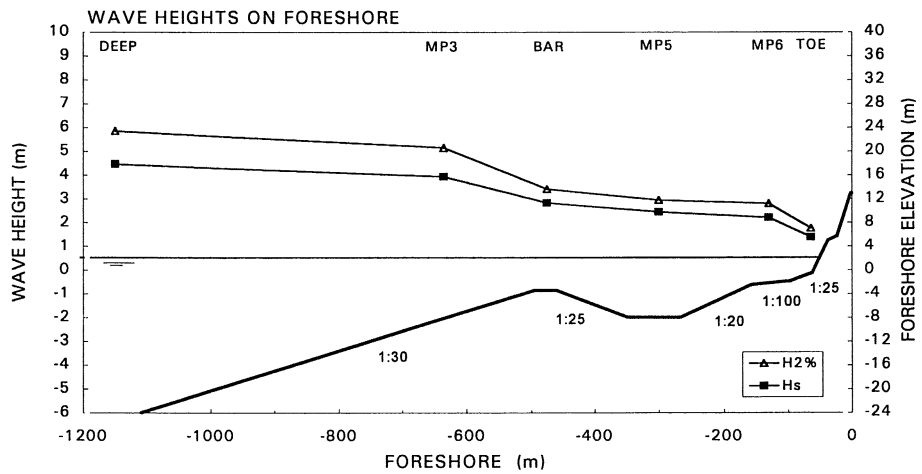
Figure 1.4 Measured wave height evolution over the foreshore.
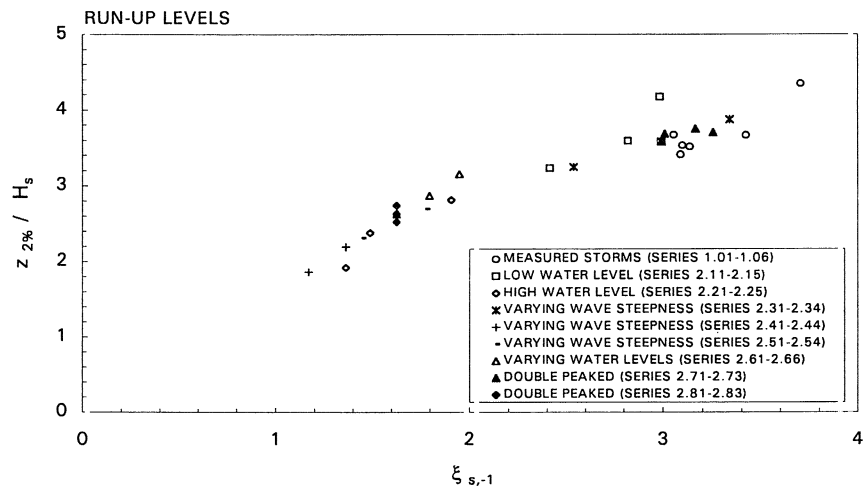
RUN-UP LEVELS

Figure 1.5 Measured 2% wave run-up levels.

SURFACE ELEVATION ON STRUCTURE
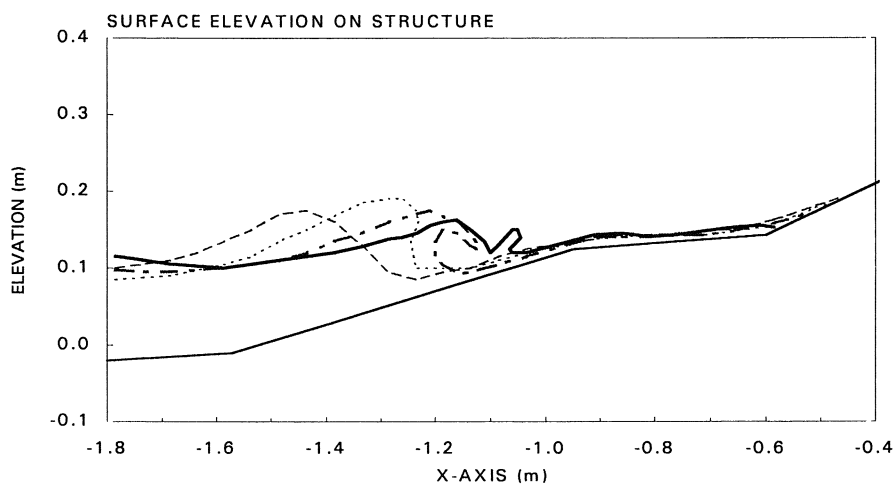
Figure 1.6 Measured surface elevations on the dike.

Test-results showed a considerable amount of wave energy in the low frequencies. Figure 1.3 shows an example of measured wave energy spectra at several locations on the foreshore. This figure shows that from deep water towards the toe of the structure the amount of energy in the short waves reduces while the amount of wave energy in the long waves increases. Both phenomena are due to wave breaking (of the short waves). Figure 1.4 shows an example of the measured wave height evolution over the foreshore which clearly indicates the reduction in wave height due to wave breaking at the bar and the shallow part in front of the dike. The resulting wave motion on the foreshore was studied by analysis of the wave run-up levels exceeded by 2% of the waves. These are shown in Figure 1.5 as function of the surf-similarity parameter (irregular waves). Figure 1.6 shows an example of the measured surface elevations on the dike (regular waves).

Test results were also obtained by performing tests without the structure in position; this to obtain mainly incident waves at the toe of the structure without large contributions of reflected waves in the total surface elevations.

A more detailed description of the model set-up, the test-results and the analysis of wave height distributions and wave run-up levels can be found in Van Gent (1999-b).

1.4   Outline

The numerical modelling of wave propagation over the shallow foreshore of Petten with the spectral wave model SWAN is described in Chapter 2. Applications of the time-domain Boussinesq-type model TRITON on shallow foreshores are described in Chapter 3.

The numerical modelling of wave motion on the sea-defence with the numerical model ODIFLOCS is described in Chapter 4. Finally, Chapter 5 provides an overview of the main conclusions with suggestions for further investigations and further development of numerical models.

2 Foreshore: Spectral wave model

2.1 Description of numerical model

The numerical model applied in this chapter is a one-dimensional version of a spectral wave model which can simulate the wave propagation over foreshores. The model (SWAN) is described in, amongst others, Ris (1997). In this section a short description of basic aspects is given.

For modelling wave propagation in coastal regions two main types of models can be distinguished, spectral wave models and time-domain models. Spectral wave models are generally applied for larger computational regions since phase-averaging can reduce the computational efforts considerably compared to time-domain model that simulate each time-increment of each individual wave. This may however cause that valuable time-information is lost such as time-signals and consequently also individual wave height statistics. Other processes that become more difficult to model are diffraction and the interaction between long waves and short waves since no distinction between bound-long waves and free long waves is made. Nevertheless, many procedures have been developed to diminish the effects of these shortcomings, resulting in a wider field of application. One of the most advanced spectral wave models is the model SWAN (Simulating WAves Nearshore). Therefore, this model has been applied here.

This spectral wave model has been designed to simulate and predict near-shore waves in deep, intermediately shallow and shallow water. The model is suitable for obtaining realistic estimates of random, short-crested wind-generated waves in complex field conditions, which may include also estuaries, tidal inlets and barrier islands with tidal flats. The model can be used in a stationary and in a non-stationary mode, of which the second mode enables modelling of changes in the spectral shape in both time and space. The model is based on the discrete spectral action balance equation and is fully spectral (over the total range of frequencies and over 360°). Wave propagation is based on linear wave theory, including the effects of currents. The processes of wave generation by wind, dissipation and non-linear wave-wave interactions are represented explicitly with source terms in the wave action balance equation. The most important physical processes accounted for are:
- *generation* of wave energy by wind,
- *dissipation* of wave energy by white-capping, depth-induced breaking and bottom friction,
- *redistribution* of wave energy of the spectrum by non-linear wave-wave interactions (both quadruplets and triads),
- *propagation* of wave energy accounting for shoaling and refraction due to currents and depth, wave blocking and wave reflection of waves by currents, and frequency shifting due to currents and depth variations.

The most important processes that are not modelled are wave diffraction, wave reflection by structures and beaches and bound long waves.

The physical processes are modelled by solving a spectral action balance equation which describes the evolution of the action density spectrum (i.e. the energy density spectrum as function of the wave direction θ and the relative frequency σ, divided by the relative frequency: $N(\sigma, \theta) = E(\sigma, \theta)/\sigma$):

$$\frac{\partial}{\partial t} N + \frac{\partial}{\partial x} c_x N + \frac{\partial}{\partial y} c_y N + \frac{\partial}{\partial \sigma} c_\sigma N + \frac{\partial}{\partial \theta} c_\theta N = \frac{S}{\sigma} \tag{2.1}$$

with

$$c_x = \frac{d x}{d t} = \frac{1}{2}\left[1 + \frac{2 k d}{\sinh 2 k d}\right]\frac{\sigma k_x}{k^2} + U_x \tag{2.2}$$

$$c_y = \frac{d y}{d t} = \frac{1}{2}\left[1 + \frac{2 k d}{\sinh 2 k d}\right]\frac{\sigma k_y}{k^2} + U_y \tag{2.3}$$

$$c_\sigma = \frac{d \sigma}{d t} = \frac{\partial \sigma}{\partial d}\left[\frac{\partial d}{\partial t} + \overline{U} \cdot \nabla d\right] - c_g \overline{k} \cdot \frac{\partial \overline{U}}{\partial s} \tag{2.4}$$

$$c_\theta = \frac{d \theta}{d t} = -\frac{1}{k}\left[\frac{\partial \sigma}{\partial d}\frac{\partial d}{\partial m} + \overline{k} \cdot \frac{\partial \overline{U}}{\partial m}\right] \tag{2.5}$$

where $c_g = \partial \sigma / \partial k$, $\overline{k} = (k_x, k_y)$ is the wave number with magnitude k, $\overline{U} = (U_x, U_y)$ is the current velocity, d is the water depth and s and m are the space co-ordinates in the wave direction θ and normal to θ respectively. In the formulations for the source term S in the action balance equation the effects of wave generation, wave dissipation and non-linear wave-wave interactions are accounted for. The formulations and the values for the involved coefficients for these source terms are under further development. Here, those described in Ris *et al.* (1998) are applied, with values for the coefficients denoted as default settings.

The numerical schemes are implicit upwind schemes in both geographic and spectral space, supplemented with a central approximation in spectral space. The model makes use of the so-called 'four-sweep technique'. In this technique, the total range of wave directions is split into four sectors of 90°, which are computed one after the other before going to the next iteration step. Computational grids, bottom and other grids can be Cartesian or curvilinear. For the computations described in the following section this is not relevant since a one-dimensional version has been applied. The use of the one-dimensional version in a steady-state mode also means that Equation 2.1 significantly reduces, because the first, third, fourth and fifth term become zero or negligibly small.

2.2 Description of numerical model computations

As described in the previous section, the spectral wave model cannot model wave reflection by dikes. Therefore, to validate the model for the present situation with a complex

foreshore, only tests where no structure was present in the flume are used (20 tests). Wave energy spectra measured in the flume at the start of the foreshore, corresponding to a location 1300 m seaward of the crest of the dike on prototype-scale, were prescribed in the computations as incident wave energy spectra. The measured wave energy spectra were obtained from measured recordings of the surface elevations. Although the structure was not present in the flume, wave reflection by the foreshore itself still affects these surface elevations. Alternatively, the surface elevations could be corrected for by methods to eliminate the reflected waves from the recordings of the surface elevations. This has not been done because these methods involve loss in resolution of the spectrum. For the validation of the applied model the effects of reflected waves in the surface elevations at deep water were considered as less important than the loss of spectral resolution. Thus, the measured surface elevations that were used for comparisons are those from individual wave gauges in tests without the structure in position. Not only the wave energy spectra are used for comparison, also the wave parameters H_{m0}, $T_{m-1,0}$ and T_p. Because the measurements involve a relatively large amount of energy in long waves which are not modelled by the numerical model, the parameters from the measurements and the numerical model used for comparisons are based on the energy in the short waves only: between the frequencies 0.04 Hz and 0.3 Hz, using exactly the same software to obtain these parameters.

Some essential parameters used in the computations with the spectral wave model SWAN (Version 30.75) are given: For the physical process the default settings were used for wave breaking (depth-induced wave breaking and whitecapping), wave set-up, bottom friction and modelling triad wave-wave interaction. Quadruplet wave-wave interactions were not modelled. The constant space step was 10 m. The spectral resolution was 73 within the frequency range between 0.04 Hz and 0.35 Hz ($\Delta f/f=0.03$) and 60 in the directional sector between -7.5 and +7.5 degrees. In all computational points a numerical accuracy of 1E-5 was required for each of the three accuracy criteria for the iteration procedure, with a maximum of 15 iterations. The above mentioned settings were used without calibration to the specific application studied here.

2.3   Comparisons with physical model tests

For each of the 20 tests used for comparisons, the measured and computed wave energy spectra at five positions on the foreshore are studied: The positions are denoted by DEEP, MP3, MP5, MP6 and TOE (see Figure 1.1 or Figure 1.4). Figures F2.1a-d in the Appendix 'Figures' show for each test these wave energy spectra. The wave energy spectra at the position DEEP are the measured wave energy spectra that were used as incident wave energy spectra for the numerical model; for this location the wave energy spectra are the same. In the measured wave energy spectra also the energy in the long waves is plotted. The wave parameters used for comparisons are not affected by this part of the wave energy spectra because this part was filtered away from the measurements before comparisons (energy in frequencies lower than 0.04 Hz). In Table T2.1 in the Appendix 'Tables' the values of the wave parameters are given for the position TOE; both the measured and computed wave parameters are based on the same frequency-range of the wave energy spectra.
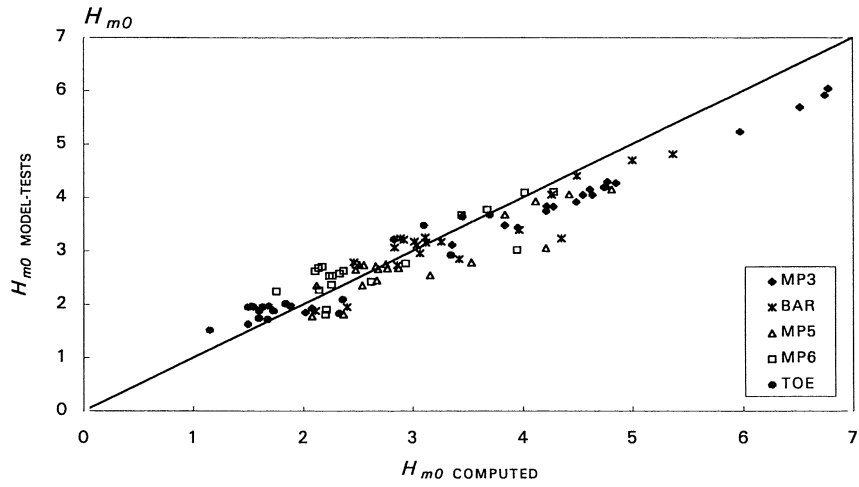
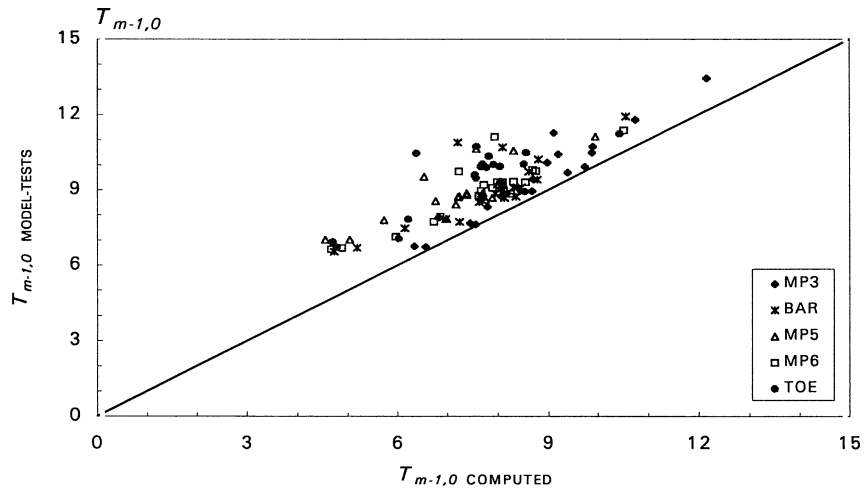Figure 2.1 Comparison between measured and computed wave heights H_{m0}.

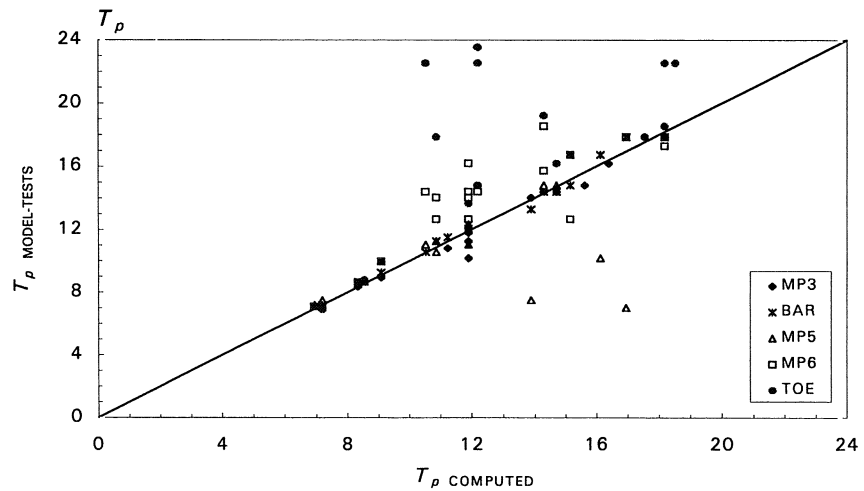Figure 2.2 Comparison between measured and computed wave periods $T_{m-1,0}$.

Figure 2.3 Comparison between measured and computed wave period T_p.

The general impression from examining Figures F2.1a-d is that the model provides realistic energy levels at all locations; the area underneath the wave energy spectra corresponding to the short waves is in general reproduced properly. Some tests show that at the first location for comparison (MP3), the total wave energy is somewhat overestimated by the model (*e.g.*, Tests 1.03 and 1.04). The modelling between deep water and this location also yields for some tests a too high shift of wave energy to higher frequencies; for some tests this results in a rather large amount of wave energy in a peak with a frequency twice the main peak (*e.g.*, Tests 2.11, 2.13 and 2.61). These differences are relatively large for tests with low water levels. Although the energy in these peaks is clearly overestimated, in locations further landward the dissipation of energy clearly reduces the amount of energy in these peaks again. Nevertheless, at the toe of the structure the numerical model shows wave energy spectra where the wave energy is still distributed in peaks at the original deep-water peak and a peak with a frequencies twice this peak, while the measurements show more flat wave energy spectra. Considering the complex foreshore with a large amount of wave energy dissipation between deep water and the toe of the structure, the model appears to be able to predict the average wave energy levels rather accurately.
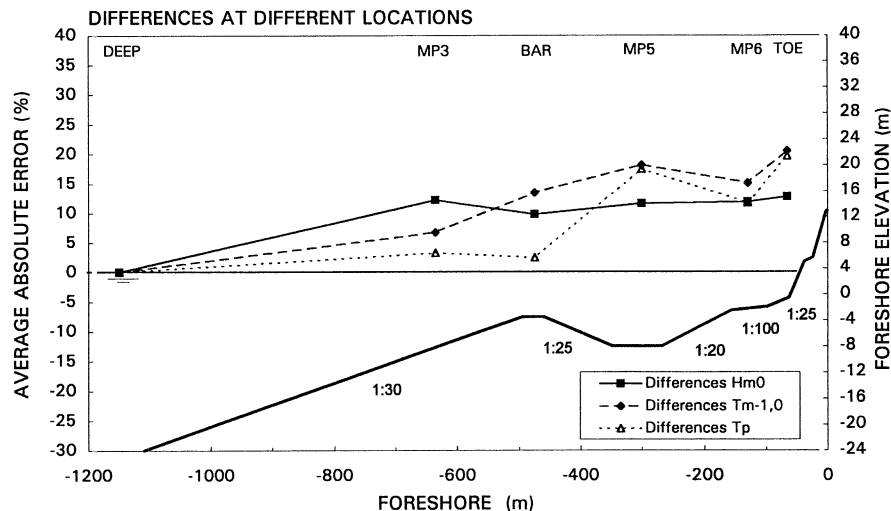
Figure 2.4 Evolution of differences in wave heights and wave periods over the foreshore.

Wave heights

Figure 2.1 shows the comparisons for the wave energy levels characterised by the wave height H_{m0}. The conclusion is that the modelling of wave propagation on the first part of the foreshore yields somewhat too high computed wave heights while at the end of the foreshore the dissipation of wave energy is too high resulting in somewhat too low wave heights. Figure 2.4 shows the evolution of the average of the absolute differences in percentage between measured and computed wave heights over the foreshore: At deep water there are no differences because the measured wave energy spectra are used as input for the computations. At the position MP3 the average differences are 12%, reduce to 10% at the crest of the bar and increase again landward to 12%, 12%, 13% at MP5, MP6 and TOE respectively. At MP3, BAR and MP5 the average differences are mainly caused by overestimates of the wave heights while at MP6 and TOE the differences are mainly caused

by underestimates of the wave heights. At the position of the toe of the structure the absolute differences are 13% on average with a standard deviation of 7%.

Wave periods

Figure 2.2 and Figure 2.3 show comparisons between measured and computed wave periods. As observed in the analysis of the shapes of the wave energy spectra, the numerical model shows too much wave energy in the higher frequencies. This kind of inaccuracies directly affects the values for $T_{m-1,0}$: As can be seen in Figure 2.2 the computed values for $T_{m-1,0}$ are systematically too low. The values for the peak wave period also show considerable deviations but for this parameter the values can be either too high or too low although at the position TOE the peak wave periods are in generally too low (Figure 2.3).

Figure 2.4 shows the differences at several locations on the foreshore. The differences for both wave periods increase with landward wave propagation. At the position TOE the differences are 21% (with a standard deviation of 8%), and 20% (with a standard deviation of 18%), for $T_{m-1,0}$ and T_p respectively.

It can be concluded from the comparisons between measured and computed wave periods that the representation of the spectral shape on such a complex foreshore apparently yields differences in wave periods which are significantly larger than the differences in wave heights.

2.4 Discussion of results

Based on the described comparisons between measurements and computations it can be concluded that the applied spectral wave model simulates the wave energy levels (wave heights) relatively accurately compared to the simulation of the spectral shape (wave periods). The differences at the position of the toe of the structure are approximately 13% on average in wave height (H_{m0}) and 20% and 21% on average in wave periods, depending on which wave period is used (T_p and $T_{m-1,0}$ respectively). For most tests the numerical model provides underestimates of the parameters. Further improvements of the spectral wave model leading to less energy transfer to higher frequencies would improve the results.

The described comparisons provide insight in the accuracy of the simulation of the propagation of short waves; the model does not provide information on the amount of energy in the long waves. Although the applied spectral wave model provides valuable insight in the propagation of short waves, additional information from other sources is required on long wave energy for processes for which long waves are important. Models such as SURFBEAT (Roelvink, 1993 and De Haas *et al.*, 1999) and Boussinesq-type models should in principle be able to also provide information on the amount of long wave energy, also for complex situations such as the present situation where a large amount of bound long wave energy becomes free due to wave breaking.

3   Foreshore: Time-domain wave model

3.1   Description of numerical model

The numerical model applied in this chapter is a time-domain model which can simulate the wave propagation over foreshores. The Boussinesq-type model TRITON developed at WL | DELFT HYDRAULICS is described briefly in this section. A more detailed description can be found in Borsboom *et al.* (2000-a,b).

Boussinesq-type wave models are in principle suitable to model wave propagation in coastal regions and harbours. Especially for the wave propagation of short waves, where non-linear effects, dispersion and shoaling play an important role, this type of model can be adequately applied and provide valuable information on the wave field which cannot accurately be obtained from many other types of models (*e.g.*, time series of surfaces and velocities in shallow regions).

Within the range of existing Boussinesq-type models, each model aims for a certain accuracy of *a)* non-linear effects, *b)* linear dispersion and *c)* shoaling. The accuracy of each of these three aspects should be in balance: Improving linear dispersion without sufficiently improving the non-linear effects might be useless if wave propagation over shallow foreshores is concerned. On the other hand, improving each of the aspects where the three aspects are in balance, might lead to a very complex model which may result in large computing times. The Boussinesq-type model applied here is a model developed to obtain an accuracy as good as possible within limited computing times. Besides a proper balance between accuracy and computing time also a proper balance was found between the accuracy of the mathematical description and accuracy of the numerical implementation. In addition, the applied model has a few unique properties for a Boussinesq-type model:

- The formulation is independent of the vertical reference level for bottom topography and water elevation, which facilitates straightforward practical applications.
- Dispersion and shoaling are modelled in a very compact way, which reduces computing times.
- Both mass and momentum are conserved, which means that the model, besides providing solutions of the applied formulations, also assures that a few basic physical properties are modelled correctly.

The equations of the 2D Boussinesq-type model, which is applied in a 1D situation here, can be written as follows:

$$\frac{\partial h}{\partial t} + \nabla \cdot \mathbf{q} = 0 \tag{3.1}$$

$$\frac{\partial \mathbf{u}}{\partial t} + \left[\nabla^{\mathrm{T}} \left(\overline{\mathbf{u}} \mathbf{q}^{\mathrm{T}} \right) \right]^{\mathrm{T}} + \nabla P = p_b \nabla h_R \tag{3.2}$$

with $\quad P = g\dfrac{\tilde{h}^2}{2}$,$\qquad p_b = g\left(\dfrac{3\tilde{h}}{2} - \dfrac{h}{2} + \dfrac{h}{4}\nabla h \cdot \nabla\zeta\right)$ (3.3)

and $\quad \tilde{h} - \alpha h^2\nabla^2\tilde{h} - \beta h\nabla h_R \cdot \nabla\tilde{h} = h + \left(\dfrac{1}{3} - \alpha\right)h^2\,\nabla^2 h + \left(\dfrac{1}{2} - \beta\right)h\nabla h_R \cdot \nabla h$ (3.4)

The unknowns in these equations are the total water depth h and the depth-integrated velocity vector $\mathbf{u}$; the bathymetry is described with respect to some arbitrary reference level h_R. From these variables the water elevation with respect to the reference level $\zeta = h\text{-}h_R$ and the depth-averaged velocity vector $\bar{\mathbf{u}} = \mathbf{q}/h$ are obtained. Auxiliary variable $\tilde{h}$ is a function of h, defined implicitly by Equation 3.4. This equation realises a so-called [2,2] Padé approximation of linear dispersion and the first order effect of linear shoaling that can be adjusted by respectively α and β. The value of these parameters should be 0.4 or slightly lower. Auxiliary variables P and p_b have been introduced because of their physical meaning. From the conservative form of momentum equation (3.2) it can be seen that P and p_b must represent respectively the depth-integrated pressure and the pressure at the bottom, both divided by the density that is assumed constant.

Wave breaking is implemented based on a new method by Borsboom where wave breaking is modelled as an eddy-viscosity model in combination with a surface roller. Wave breaking is implemented as an eddy-viscosity model as for instance also applied by Kennedy et al. (2000):

$$\frac{\partial}{\partial x_w} h\nu_t \frac{\partial \bar{u}_w}{\partial x_w}$$ (3.5)

where x_w is the propagation direction of the wave, h is the water depth, $\bar{u}_w$ is the depth-averaged flow velocity in x_w-direction and ν_t is the turbulence-viscosity coefficient, which is uniform over the depth. For the determination of ν_t use is made of the concept of surface rollers (Schäffer et al., 1992). The idea behind this concept is as follows: Wave breaking is assumed to initiate if the slope of the local water surface exceeds a certain value for ϕ_{ini} and assumed to finish if the slope of the local water surface becomes below a certain value for ϕ_{ter}. The water above the tangent of this critical slope is assumed to belong to the roller. This slope is assumed to vary in time while being constant in space within each surface roller:

$$\tan\phi = \tan\phi_{ini} + (\tan\phi_{ter} - \tan\phi_{ini})\exp\left[-\ln 2\,\frac{t - t_b}{t_{1/2}}\right]$$ (3.6)

The turbulence-viscosity coefficient that is used in the present model is scaled with the height of this surface roller:

$$\nu_t = f_p\,\delta(c - \bar{u})$$ (3.7)

where δ is the roller height, c is the local wave celerity modelled as $c = \sqrt{gh}$ and f_p is the parameter that is used for scaling.

The model makes use of four coefficients of which the values are based on a sensitivity-analysis using a selection of tests from the present data-set. These coefficients are kept constant in all computations. The initial angle of the surface for which breaking starts ϕ_{ini} is estimated to be in the order of 15° which exponentially changes to the terminal breaking angle ϕ_{ter} which is in the order of 10°. The parameter $t_{1/2}$ is a measure related to the time required for the wave to pass through the breaking process. The following value $t_{1/2} = T_m/10$ is used. The amount of energy dissipation can be scaled with the parameter f_p for which a value of 30 has been used.

Another important aspect of the model is the modelling of weakly reflecting boundaries, based on the concepts by Borsboom et al. (2000-a,b).

3.2 Description of numerical model computations

Similar to the comparisons in Section 2.2, again 20 tests are used where no structure was present in the flume. Measured time signals of the incident waves at the start of the foreshore, corresponding to a location 1300 m seaward of the crest of the dike in prototype, were prescribed in the computations as incident waves. At this seaward wave boundary the surface elevations were prescribed while at the landward boundary (toe of the structure) an open weakly reflecting boundary was used. At this open boundary the waves can leave the computational domain, where use is made of the long-wave assumption at this boundary to assess the phase velocity of the outgoing waves. Some essential parameters used in the computations are the space-step $\Delta x = 1.0$ m and time-step $\Delta t = 0.06$ s.

For comparisons between the measured and computed wave parameters, again the measured recordings of the surface elevations of individual wave gauges are used, thus including incident and reflected waves. The wave parameters H_{m0}, $T_{m-1,0}$ and T_p are used for comparison. The same software for analysis of time-signals was used for the measured and the computed time-signals. The parameters from the measurements and the computations are based on the energy between the frequencies 0.04 Hz and 0.3 Hz. In the computations approximately 500 waves were computed which is shorter than the actual measurements, which had a duration of approximately 1000 waves. The measured and computed wave parameters were obtained from the time-series of these 500 waves.

The module for wave breaking requires calibration, in principle for each Boussinesq-type model in which it is implemented. Since this wave breaking model is applied here for the first time the parameters were calibrated based on these tests. Because these tests concern strongly breaking waves it must still be verified whether the coefficients need to be re-calibrated for situations with weakly breaking waves.

3.3   Comparisons with physical model tests

The results of the 20 tests that were performed by the time-domain model are presented in Figures F3.1a-d in the Appendix 'Figures'. As mentioned above both the computed and the measured spectral parameters were obtained from the time-series of approximately 500 waves. However, the measured wave energy spectra as shown in the Appendix 'Figures' are based on the complete measured time signals of 1000 waves, which explains the small differences between the measured and computed wave energy spectra at the location DEEP.

The general impression from examining Figures F3.1a-d is that the time-domain model simulates both the spectral shapes and the energy levels rather accurately. Also the energy shift to the lower frequencies is modelled surprisingly well (e.g., Tests 1.01, 1.02 and 2.51). Some tests in the measurements show clear peaks at low frequencies that are not that sharp in the computational results. This energy in low frequencies does not fully dissipate at the wave absorber at the rear-side of the flume and so this energy reflects for a relatively large part back into the flume; in the computations the rear-side of the flume was modelled as open which means that this reflection did not occur in the numerical model simulations, causing differences which cannot be attributed to inaccurate modelling of the wave propagation in the numerical model.

Wave heights

Figure 3.1 shows the comparisons for the wave energy levels characterised by the wave height H_{m0}. The conclusion is that the modelling of wave propagation yields somewhat too high computed wave heights. Figure 3.4 shows the evolution of the average of the absolute differences in percentage between measured and computed wave heights over the foreshore: At deep water there are no differences because the measured wave signals are used as input for the computations. At the position MP3 the average differences are 5.0%, increase to 7.4% at the crest of the bar, 7.3% at MP5 and increase again landward to 7.8%, 9.6% at MP6 and TOE respectively (with a standard deviation of 4.5% and 5.6% respectively). At all locations the average differences are caused by overestimate of the wave height.

Wave periods

Figure 3.2 and Figure 3.3 show comparisons between measured and computed wave periods. As can be seen in Figure 3.2 the differences between the measured and the computed $T_{m-1,0}$ are relatively small (4% on average). The values for the peak wave period show considerable deviations but for this parameter the values can be either too high or too low, although at the position TOE the peak wave periods are in generally too low (Figure 3.3).
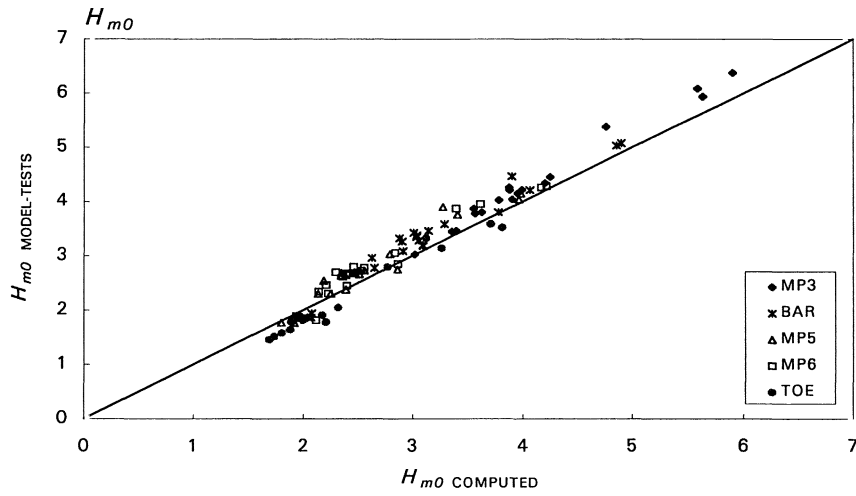
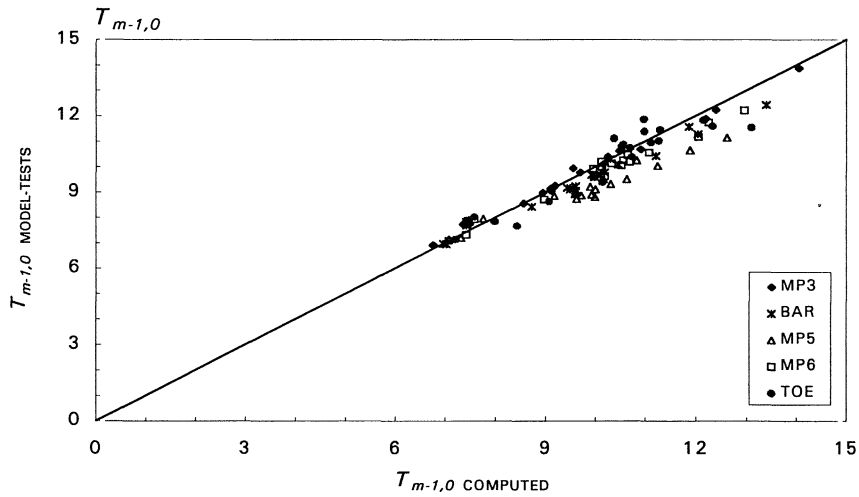Figure 3.1 Comparison between measured and computed wave heights H_{m0}.

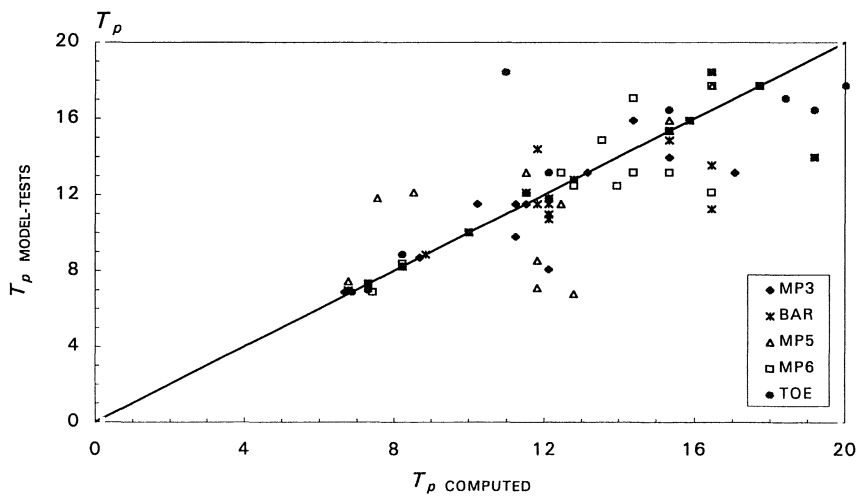Figure 3.2 Comparison between measured and computed wave periods $T_{m-1,0}$.

Figure 3.3 Comparison between measured and computed wave period T_p.

Figure 3.4 shows the differences at several locations on the foreshore. The differences for both wave periods increase with landward wave propagation. At the position TOE the differences are 4% (with a standard deviation of 3.4%) and 15% (with a standard deviation of 14.7%), for $T_{m-1,0}$ and T_p respectively.
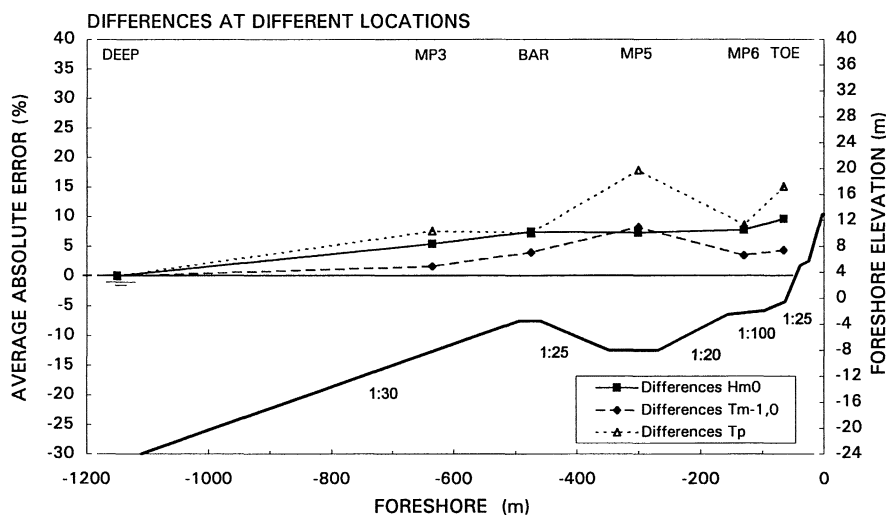
Figure 3.4 Evolution of differences in wave heights and wave periods over the foreshore.

3.4 Discussion of results

The comparisons between measurements and computations show that the applied time-domain wave model simulates the wave propagation over the foreshore, including the energy dissipation due to severe wave breaking, rather well.

The differences at the position of the toe of the structure are on average less than 10% and 5% for the wave height H_{m0} and wave period $T_{m-1,0}$ respectively, both based on the energy in the short waves only. The peak wave period is reproduced less accurate (15%). Based on the measurements alone it was already concluded that this parameter is considered as a less suitable parameter for applications with shallow foreshores (Van Gent, 1999-b). The accuracy of the predictions for the wave periods is higher than obtained with the spectral wave model, though at the cost of higher computational efforts. Because the wave height H_{m0} and wave period $T_{m-1,0}$ are the most important parameters for predictions of for instance wave run-up and wave overtopping, it can be concluded that the numerical model is suitable for applications with shallow foreshores.

Although the analysis was primarily focussed on wave energy in the short waves, it can be concluded based on visual inspections of the measured and computed wave energy spectra that transfer of energy from the short waves to the lower frequencies is modelled. Therefore, it is recommended to apply and explore the possibilities of the model to study the effects of long waves and the interaction between short and long waves (bound and unbound long waves) on coastal processes.

4 Structure:
Shallow-water wave equation model

4.1 Description of numerical model

The numerical model applied in this chapter is a time-domain model which can simulate the wave motion on the slope of coastal structures. The model (ODIFLOCS) is described more in detail in Van Gent (1994, 1995). In this section a short description of basic aspects is given.

The model allows for simulations of normally incident wave attack on various types of structures. Use is made of the non-linear shallow-water wave equations where steep wave fronts are represented by bores. The model is based on concepts by Hibberd and Peregrine (1979) who developed a numerical model with an explicit dissipative finite-difference scheme (Lax-Wendroff) for impermeable slopes without friction. Using this concept, many practical applications have been obtained. See for instance Kobayashi *et al.* (1987) for wave reflection and run-up on impermeable rough slopes. In Van Gent (1994, 1995) these concepts are used and extended such that the model allows for simulations of the wave interaction with permeable coastal structures. The model consists of two coupled regions; one for the external wave motion and one for permeable part. The basic equations of the model for the two regions are:

External wave motion:

$$\frac{\partial h u}{\partial t} + \frac{\partial h u^2}{\partial x} = -g h \frac{\partial h}{\partial x} - g h \tan \varphi_s - \frac{1}{2} f u |u| + q q_x \qquad (4.1)$$

$$\frac{\partial h}{\partial t} + \frac{\partial h u}{\partial x} = q \qquad (4.2)$$

Internal wave motion:

$$(1+c_A)\frac{\partial hu}{\partial t} - c_A u \frac{\partial h}{\partial t} + \frac{1}{n}\frac{\partial hu^2}{\partial x} = -ng\frac{\partial \frac{1}{2}h^2}{\partial x} - ngh\tan\varphi_c - ngh(au + bu|u|) + \frac{qq_x}{n} \qquad (4.3)$$

$$\frac{\partial h}{\partial t} + \frac{1}{n}\frac{\partial h u}{\partial x} = -\frac{q}{n} \qquad (4.4)$$

where h is the thickness of the waterlayer in the corresponding region, u is the depth-averaged (filter) velocity, φ is the angle of the slope or the core inside the structure, f is the bottom friction coefficient, a, b and c_A are coefficients for the permeability and flow resistance of the permeable region, n is the porosity, q is the volume-flux of the flow between the two regions and q_x is the horizontal component of the velocity of this flow.

The model is able to deal with either regular or irregular waves which attack various types of structures with arbitrary seaward slopes, smooth or rough, permeable or impermeable, overtopped or not. Since the non-linear shallow-water wave equation overestimates the non-linear effects, because these effects are not counteracted by frequency dispersion, inaccuracies will occur when wave propagation over long distances is concerned. Therefore, for many applications it is advisable to start the wave simulations at the toe of the structure. On the slope itself the distances are relatively small and non-linear effects are more important than frequency dispersion. Many applications show that sufficiently accurate results can be obtained for many types of applications. The model is applied here because earlier computations already showed that the model can be applied successfully for sensitivity analyses on the effects of wave energy spectra on wave run-up and wave overtopping (Van Gent, 1999-a).

The model allows for wave generation with arbitrary wave energy spectra. The time-series can be generated using random phases. Also recordings of measured surface elevations can be generated as incident wave trains. At the incident wave boundary reflected waves are allowed to leave the computational domain by assuming linear long waves at this boundary. These assumptions are unlikely to be valid at the toe of a structure. The effects of this assumption and other approximations can be studied by validations with analytical solutions and test-results from physical models. In addition to validations described in Van Gent (1994, 1995), here additional comparisons with physical model tests are performed.

4.2 Description of numerical model computations

Two sets of computations have been performed for validation based on the physical model tests on the Petten Sea-defence. The first set concerns computations with regular waves, mainly for comparisons between measured and computed surface elevations (derived from Beck, 1999). The second set concerns computations with irregular waves for comparisons between measured and computed wave run-up levels.

Surface elevations

Four tests with regular waves were performed while the surface elevations on the slope were recorded using a video. Table 4.1 shows the conditions for these tests.

No	SWL (NAP)	H_{DEEP}	T	s_{DEEP}	$H_{COMPUTATIONS}$
3.91	4.7	4	6	0.071	2.2
3.92	4.7	4	8	0.040	2.3
3.93	4.7	4	10	0.025	2.2
3.94	4.7	4	12	0.018	1.9

Table 4.1   Tests with regular waves for validation of surface elevations.

For eight moments in time within a wave period, with a constant time-interval, the surface profile were obtained from the video-recordings. Beck (1999) performed computations for comparison between measured and computed surface elevations. The basic input for these

computations is summarised here. Because the model is in principle not suitable to compute the wave motion over the foreshore, the incident wave boundary in the computations was taken at about 10 m seaward of the toe of the dike. Neither at this particular location, nor at the toe of the dike, wave height recordings were made for these tests; the wave height of the incident waves was obtained based on an analysis of the measured wave height at a more seaward location (MP6). The wave height used in the computations are given in the last column of Table 4.1. For other input parameters the following values were used by Beck (1999) in all computations, which were done on the scale of the prototype situation: Δx=0.5 m (space step), Δt=0.025 s (time-step) and f=0.1 (friction coefficient). After reaching a periodic situation in the computations, the surface elevations and the maximum wave run-up levels were used for comparison with the test-results.

Wave run-up

All tests with irregular waves where also tests without the structure in position are available, were used for comparison. For five of the 20 tests the wave run-up levels were either below the upper berm (see Figure 1.2), where no measurements were performed, or above the crest.

Three sets of computations are performed with three different sources to obtain incident waves in the computations:
A)   Measured surface elevations of incident waves,
B)   Computed surface elevations derived from the spectral foreshore model,
C)   Computed surface elevations from the time-domain foreshore model.

The first data-source is in principle the data-source to select if all three options are available. However, here the incident waves from the numerical models, modelling the wave propagation over the foreshore, are also applied to obtain insight in the accuracy of the predictive models for situations in which no measurements would be available. In all three situations only the surface elevations are given while the corresponding velocities are computed based on the long-wave assumption as used by the applied model for wave interaction with the structure. In the computations approximately 500 waves were computed which is shorter than the actual measurements, which had a duration of approximately 1000 waves. The measured and computed wave parameters were obtained from the time-series of these 500 waves.

In the computations the lower 1:4.5 slope was extended tot a depth equal to the depth of the trough between the bar and the toe of the structure. This extension to deeper water was used because the depth at the toe is so small that in some situations at this position there is no water or almost no water present for a part of the wave cycle; it would therefore be hard or impossible to place the incident wave boundary at such a position. For the most important input parameters the following values were used in all computations, which were done on the scale of the prototype situation: Δx=0.8 m (space step), Δt=0.01 s (time-step) and f=0 (friction coefficient). This means that the slope is modelled as smooth (no friction). The computed wave run-up levels exceeded by 2% of the incident waves are those with water-layers thicker than 0.10 m. This is equal to the required thickness in the physical model tests to obtain results with the step-gauge (see Van Gent, 1999-b).

The results of the wave run-up computations are given in Table T4.1-T4.3 (in the Appendix 'Tables'). The tables show parameters of the incident waves (H_s, T_p and $T_{m-1,0}$) and the wave run-up levels exceeded by 2% of these incident waves ($z_{2\%}$).

4.3 Comparisons with physical model tests

Surface elevations

The computations with regular waves, as briefly discussed in the previous section, were performed to compare the measured surface elevations. Figures F4.1-F4.4 (in the Appendix 'Figures') show the measured and computed surface elevations for eight moments within a wave cycle with a constant time-interval. The comparisons show that the overturning of the waves as occurs in each of these tests cannot be modelled with this one-dimensional wave model. The comparisons, especially for the first test (Test 3.91), nevertheless show that the model can provide a useful impression of the wave motion on the slope. Except for the overturning wave tongue, the main differences are caused by the wave front above the berm which propagates slower in the computations than in the measurements. The wave run-up levels are underestimated (see Beck, 1999), these differences reduce if no friction ($f=0$) would have been applied.

Wave run-up

The computations with irregular waves, as discussed in the previous section, are performed to compare measured and computed wave run-up levels. Three sets of computations are performed with different sources for the incident waves. Figures 4.1-4.3 show the comparisons between the measured and computed wave run-up level, each with a different source for the incident waves. All wave run-up levels are made non-dimensional with the *measured* incident wave height at the position of the toe of the structure.

Series A: Measured surface elevation as incident waves

Figure 4.1 shows that the computed wave run-up levels using the measured waves as incident waves are lower than the measured wave run-up levels. On average the computed wave run-up levels are 10% lower than the measured wave run-up levels. These differences are rather systematic since the deviations from the line '$y=1.1\ x$' (Figure 4.1) are relatively small (a standard deviation of 4%). For a few tests the wave run-up levels were above or below the slope-section in which the measurements took place; the corresponding computations also gave wave run-up levels which were either below or above this slope-section.
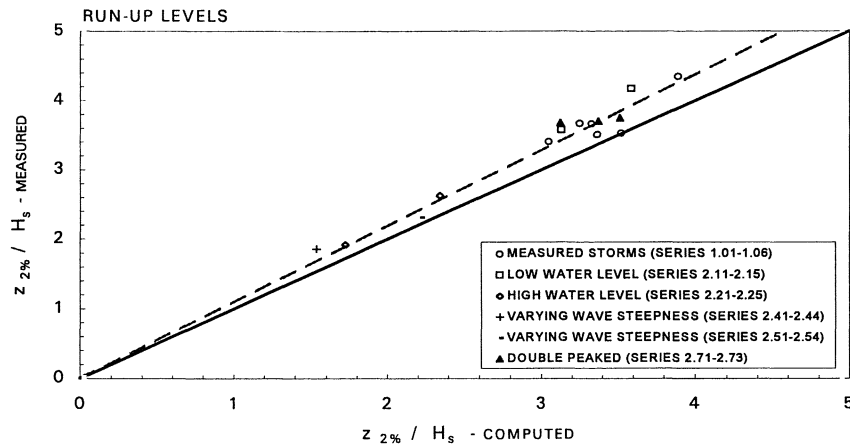
RUN-UP LEVELS

Figure 4.1 Comparison between measured and computed wave run-up levels, with incident waves from measurements (the dashed line '$y=1.1\,x$' denotes the average difference).

RUN-UP LEVELS

Figure 4.2 Comparison between measured and computed wave run-up levels, with incident waves derived from the spectral foreshore model (the dashed line '$y=1.18\,x$' denotes the average difference).

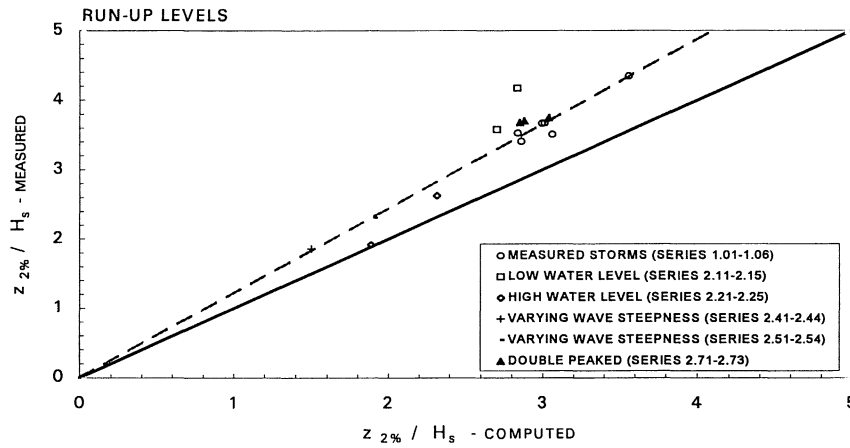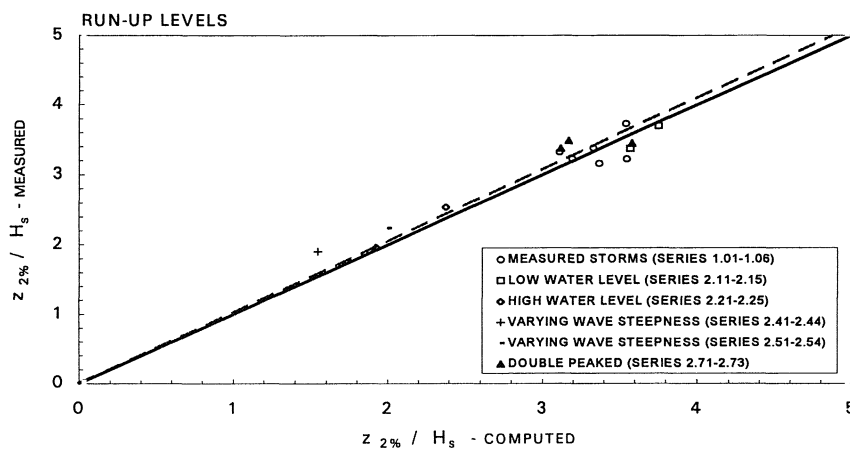RUN-UP LEVELS

Figure 4.3 Comparison between measured and computed wave run-up levels, with incident waves derived from the time-domain foreshore model (the dashed line '$y=1.03\,x$' denotes the average difference).

A few explanations can be given for the observed differences between measured and computed wave run-up levels.

- In the numerical model the amount of energy-dissipation depends on the numerical dissipation; this numerical dissipation, which occurs especially at the wave front where in reality wave breaking occurs, apparently is for these situations stronger than the energy dissipation due to wave breaking. These differences in energy dissipation due to numerical dissipation in the model and wave breaking in reality become relatively important in this situation because other energy dissipation mechanisms such as friction are relatively small.

- Although the measured signal of the surface elevations of the incident waves is generated, still the model uses the assumption of long waves at the incident wave boundary to obtain a corresponding velocity. The assumptions of long waves in general causes differences between the measurements and the computational results.

- The measured wave signals of the surface elevation at the position of the toe of the structure were used in the computations. These signals originate from tests without the structure in position. This means that in fact the assumption is made that the structure does not influence the signals of the incident waves at this position. It is however likely that to some extent the structure affects the incident waves at the toe of the structure because of interaction between the incident waves and the waves reflected by the structure. This causes differences in the wave signals at the toe between the tests without the structure in position and the tests with the structure in position, and consequently, also between the measured wave run-up levels and the computed wave run-up levels.

Series B: Computed surface elevations from spectral model as incident waves

The spectral wave model used for modelling wave propagation over the foreshore does not provide time-signals of surface elevations which can be used as input for the wave run-up model. Therefore, output from the spectral wave data needs to be translated into time-signals.

The signals of the surface elevations obtained from the spectral wave model are derived with the assumption of 'random phases' and assuming a deep-water (Rayleigh) wave height distribution. The wave height distribution at the toe deviates from the deep-water situations such that using the Rayleigh distribution leads to wave signals in which the extreme wave heights (*e.g.*, $H_{2\%}$) are somewhat higher than if the correct wave height distribution would be applied. A method to obtain wave signals with a prescribed distribution such as distributions obtained from the method described in Groenendijk and Van Gent (1998) is not available. This means that the transfer from output of the spectral 'foreshore model' SWAN to input for the 'structure model' ODIFLOCS, yields somewhat too high extreme wave heights. Differences between measurements and computational results therefore originate from three basic sources: a) modelling wave propagation over the foreshore (SWAN), b) transfer from spectral wave information to time-domain information and c) modelling the wave interaction with the structure (ODIFLOCS). The first source of differences can be characterised with a mean difference between measured and computed H_{m0}, *i.e.* an *underestimate* of 13% (*i.e.*, results from Chapter 2), the second source can be characterised by an *overestimate* of the ratio $H_{2\%}/H_{m0}$ of 6% compared to the measurements and the third

source can be characterised by the *underestimate* of 10% of the wave run-up levels computed, with measured wave signals at the toe as input, compared to the measured wave run-up levels (*i.e.,* the results from Series A).

Figure 4.2 shows the computational results with the above described approach. The computed wave run-up levels are on average 18% lower than the measured wave run-up levels, with a standard-deviation of 6%. In Figure 4.2 the wave run-up levels are made non-dimensional with the *measured* wave height at the toe. The magnitude of the differences indicates that the modelling of the wave interaction with the structure (10% underestimate) and the modelling of wave propagation over the foreshore together with the transfer from spectral wave data to time-signals equally contribute to the resulting overall average underestimate of the wave run-up levels (18%).

Series C: Computed surface elevations from time-domain model as incident waves

The time-domain wave model used for modelling wave propagation over the foreshore provides time-signals of surface elevations which can be used as input for the wave run-up model. To extract the reflected waves from the computed total time-signals at the toe of the structure, exactly the same method as in the measurements was applied (Mansard and Funke, 1980). This yielded the incident waves used in the computations.

Differences between measurements and computational results originate from three basic sources: a) modelling wave propagation over the foreshore (TRITON), b) extracting reflected waves from signals of total surface elevation, and c) modelling the wave interaction with the structure (ODIFLOCS). The first source of differences can be characterised with a mean difference between measured and computed H_{m0}, *i.e.* an *overestimate* of 10% (*i.e.,* results from Chapter 3), the second source does not decrease the accuracy compared to the computations with incident waves from the measurements (Series A) and the third source can be characterised by the *underestimate* of 10% of the wave run-up levels computed, with measured wave signals at the toe as input, compared to the measured wave run-up levels (*i.e.,* the results from Series A).

Figure 4.3 shows the computational results with the above described approach. The computed wave run-up levels are on average 2% lower than the measured wave run-up levels, with a standard-deviation of 8% (the average of the absolute values of the errors is 6%). In Figure 4.3 the wave run-up levels are made non-dimensional with the *measured* wave height at the toe. The magnitude of the differences indicates that the modelling of the wave interaction with the structure (10% *underestimate*) and the modelling of wave propagation over the foreshore (10% *overestimate*) to a large extent counteract each other since the overall average differences of the wave run-up levels is very small (less than 3%).

The average differences between the measured and computed wave run-up levels with the corresponding standard deviations are given in Table 4.2.

Data set	differences $\Delta z_{2\%}/H_s$	standard deviation
Measured incident waves	9.7%	4.4%
Incident waves from spectral foreshore model	18.2%	6.4%
Incident waves from time-domain foreshore model	2.7%	7.4%

Table 4.2   Comparison between measured and computed wave run-up levels.

The measured wave run-up levels can be described by using the following formula (Van Gent, 1999-a) with the values c_0=1.55 and c_1=5 (these values depend strongly on the applied filtering; no filtering at all yields c_0=1.25 and c_1=4.1):

$$z_{2\%} / (\gamma \, H_s) = c_0 \, \xi_{s,-1} \qquad \text{for } \xi_{s,-1} \le p$$

$$z_{2\%} / (\gamma \, H_s) = c_1 - c_2 / \xi_{s,-1} \qquad \text{for } \xi_{s,-1} \ge p \qquad (4.5)$$

where continuity between both sections and their derivatives determine c_2=0.25 c_1^2/c_0 and p=0.5 c_1 / c_0. The wave height and wave period are those at the toe of the structure. The surf-similarity parameter was defined as $\xi_{s,-1}$ = tan φ / $\sqrt{(2\pi/g \cdot H_s /T_{m-1,0}^2)}$. No reduction for friction or other influences has been applied (γ=0). The computational results can best be described with the values c_0=1.4 and c_1=4.5 (with a standard deviation of 0.18), which are about 10% lower than those for the measurements because the computed wave run-up levels are about 10% lower. The characteristic slopes in the surf-similarity parameter are computed with the method described in Van Gent (1999-b): The characteristic slope φ is the average slope between the two positions on the slope with a level of two wave heights below still water and a level of two wave heights above still water. Figure 4.4 shows the computational results compared to Equation 4.5 with the above mentioned coefficients. The two tests with the largest deviation from the trend are the same two tests for which also the measured wave run-up levels deviate the most from the trend.

RUN-UP LEVELS

o MEASURED STORMS (SERIES 1.01-1.06)
□ LOW WATER LEVEL (SERIES 2.11-2.15)
◇ HIGH WATER LEVEL (SERIES 2.21-2.25)
+ VARYING WAVE STEEPNESS (SERIES 2.41-2.44)
- VARYING WAVE STEEPNESS (SERIES 2.51-2.54)
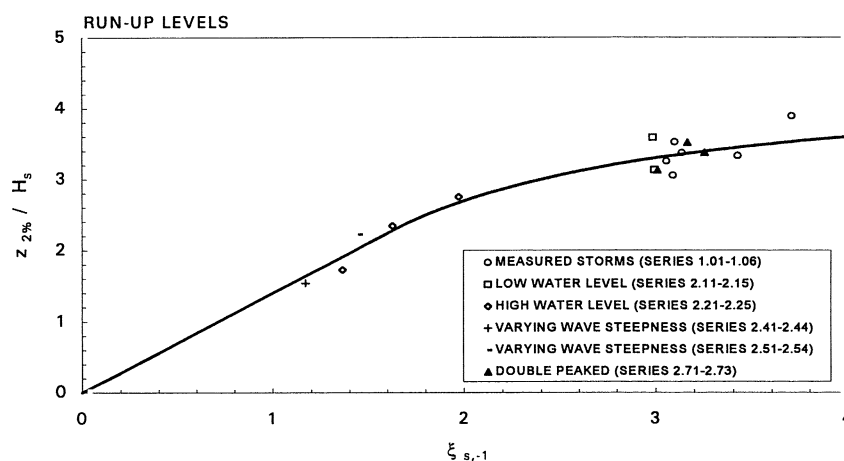▲ DOUBLE PEAKED (SERIES 2.71-2.73)

Figure 4.4   Computed wave run-up levels and the corresponding calibration of Equation 4.5.

4.4   Discussion of results

Although the comparison of surface elevations on the slope indicates that the model may provide useful impressions of the wave motion on the slope, here the wave run-up level is the main parameter for validation. The main conclusions from the comparisons between the measured and computed wave run-up levels are:

- The dependency on the surf-similarity parameter, as observed in the measurements is equally well represented by the computational results.

- On average the computed wave run-up levels are lower than the measured wave run-up levels (10% difference); together with the proper representation of the dependency on the surf-similarity parameter it can be concluded that the numerical model for wave interaction with structures is for many situations a valuable research-tool and design-tool.

- Modelling the wave propagation over the foreshore with the applied spectral wave model to obtain waves at the toe of the structure, doubles the mean differences between measured and computed wave run-up levels; the wave run-up predictions based on the combination of these two numerical models result in an underestimate of 18% on average. Unlike the computations where measured time-signals or the computed time-signals from the time-domain model were used as input, the time-series derived from this spectral wave model do not contain long waves. Although in the analysis of the waves only the energy in the short waves was regarded, it is expected that wave run-up levels are affected by these long waves. This is considered as one of the reasons why the computations with input derived from the spectral wave model provides lower run-up levels.

- Modelling the wave propagation over the foreshore with the applied time-domain model to obtain waves at the toe of the structure, results in differences of 3% on average between measured and computed wave run-up levels. This relatively good performance of the combination of these two numerical models is partly due to counteracting inaccuracies; the 'foreshore models' yield too little energy dissipation while the 'structure model' yields too much energy dissipation.

The overall conclusion is that both the representation of the trend and the quantitative results are sufficiently modelled to apply the model for wave interaction with structures as a tool to provide valuable insight in wave run-up levels. Also the combination with numerical models modelling the wave propagation over the foreshore may provide sufficiently accurate estimates. Nevertheless, improvements of each of the applied numerical models may further increase the accuracy of the predictions.

5   Conclusions and recommendations

Based on the investigations described in this report the following conclusions and recommendations can be given:

Conclusions:

- Three numerical models have been applied for validation based on test results from 2D-physical model investigations with a shallow foreshore in front of a dike. The 20 tests with rather wide variations in parameters concern wave propagation over the shallow foreshore, with a shallow bar, several breaker zones, non-standard wave energy spectra and large amounts of energy in low-frequencies, which is considered as relatively difficult for numerical models to simulate. The wave interaction with the dike concerns wave breaking in a situation with a berm.

- The spectral wave model, applied for wave propagation of short waves over the foreshore (SWAN), yields valuable impressions and insight in the evolution of wave energy spectra over the foreshore. It also shows that the computed energy levels in the short waves are rather accurately predicted, considering the rather extreme energy dissipation in the tests. The wave parameters H_{m0} and $T_{m-1,0}$ at the toe of the structure are both underestimated (13% and 21% respectively), using the default-settings of this numerical model. Modifications of the numerical-model settings for this kind of applications might improve the comparisons. Further improvements of this model could be dedicated to decrease the wave energy transfer to higher frequencies and to increase the wave energy transfer to lower frequencies.

- The time-domain wave model applied for wave propagation over the foreshore (TRITON) shows accurate results for the wave parameters H_{m0} and $T_{m-1,0}$ at each position. The deviations at the toe of the structure are the largest but still remain below 10% and 5% respectively (based on the energy in the short waves). The evolution of the wave energy spectra is also rather accurately simulated, despite the extreme energy dissipation. Also the energy transfer to lower frequencies is clearly present and considered as accurately modelled. The model to include wave breaking in this Boussinesq-model shows to be highly effective in reducing the wave energy without significant loss of accuracy in the simulation of wave energy spectra. Further improvements of this model could be dedicated to obtain results with a similar accuracy for 2DH-situations with angular wave attack, directional spreading and non-uniform depth-contours.

- The time-domain wave model applied for wave interaction with the dike (ODIFLOCS) shows that valuable results on wave run-up levels can be obtained if use is made of measured surface elevations of the incident waves (on average 10% underestimate of the wave run-up levels). Using incident waves based on numerical results from the spectral wave model (SWAN) doubles the mean differences (18%) because both numerical models lead to too much wave energy dissipation compared to the measurements. Using incident waves based on numerical results from the time-domain wave model (TRITON) reduces the differences significantly (on average less than 3%) because the numerical models provide counteracting errors: The foreshore-model shows too little dissipation while the

structure-model shows too much dissipation. Nevertheless, applying the two models together led to relatively accurate predictions of the wave run-up levels for the present data-set.

5 – 2

Recommendations:

- Considering that the shallow foreshore with a bar as used here is a rather common situation, for instance along the Dutch coast, and that each of the models is valuable for practical situations, it is advised to *validate*, and if necessary and possible *calibrate* or *improve*, the three applied numerical models for different foreshore configurations and dike geometries.
- For future applications it might be valuable to use the relatively fast 2DH-spectral model SWAN along coasts and in estuaries providing boundary conditions for the relatively slow and accurate time-domain model TRITON, which is then used for computing the wave propagation in the shallow regions. This model on its part provides boundary conditions for computing the wave dynamics on coastal structures. Therefore it is advised to further investigate methods for *coupling* two models.
- The results presented in this report were mainly focussed on the energy in the short waves. It is expected that further improvements of the spectral wave model will for most situations, with bound and unbound long waves in shallow regions, not result in sufficiently accurate simulations of long waves. The time domain wave model however is in principle suitable to simulate and study the *long and short waves* in a wave field and the interactions between both. Therefore it is advised to use this model also for studying long wave phenomena and their effects on coastal processes and hydrodynamic boundary conditions for coastal structures.

Acknowledgements

References

Battjes, J.A. and H.W. Groenendijk (1999), *Shallow foreshore wave height statistics*, Proc. Coastal Structures 1999, Santander, Spain.

Beck, S.C. (1999), *Investigations on two aspects of the Petten Sea-defence model tests*, Study-paper at Delft Hydraulics as visiting researcher from Leichtweiss Institut für Wasserbau, Braunschweig/Delft.

Borsboom, M.J.A., J. Groeneweg, N. Doorn and M.R.A. van Gent (2000-a), *Boundary conditions for a 2D Boussinesq-type wave model*, Delft Hydraulics Report H3581-January 2000, Delft.

Borsboom, M.J.A., J. Groeneweg, N. Doorn and M.R.A. van Gent (2000-b), *A Boussinesq-type wave model that conserves both mass and momentum*, Paper accepted for presentation/publication at ICCE 2000, Sydney.

De Haas, P.C.A., D.C. Rijks, B.G. Ruessink, J.A. Roelvink, A.J.H.M. Reniers, M.R.A. van Gent (1999), *Onderzoek naar lange golven bij Petten (in Dutch); Investigations on long waves at Petten*, Report by University Utrecht and Delft Hydraulics, Report H3345-January 1999, Delft.

Groenendijk, H.W. and M.R.A. van Gent (1998), *Shallow foreshore wave height statistics; A predictive model for the probability of exceedance of wave heights*, Delft Hydraulics Report H3351-October 1998, Delft.

Groenendijk, H.W. (1998), *Shallow foreshore wave height statistics*, M.Sc.-thesis, Delft University of Technology, Also: Delft Hydraulics Report H3245-February 1998, Delft.

Hibberd, S. and D.H. Peregrine (1979), *Surf and run-up on a beach: a uniform bore*, J. of Fluid Mechanics, Vol.95, part 2, pp.323-345.

Kennedy, A.B., Q. Chen, J.T. Kirby and R.A. Dalrymple (2000), *Boussinesq modeling of wave transformation, breaking and runup. I One Dimension*, J. of Waterway, Port, Coastal and Ocean Engrg, ASCE, Vol.126, pp.39-47.

Kobayashi, N., A.K. Otta and I. Roy (1987), *Wave reflection and run-up on rough slopes*, J. of Waterway, Port, Coastal and Ocean Engrg, ASCE, Vol.113, No.3, pp.282-298.

Luth, H.R., G.W. Klopman and N. Kitou (1994), *Project 13G: Kinematics of wave breaking partially on an offshore bar; LDV measurements for waves with and without a net onshore current*, Delft Hydraulics Report H1574-March 1994, Delft.

Mansard, E. and E. Funke (1980), *The measurement of incident and reflected spectra using a least-square method*, Proc. ICCE'80, Sydney.

Ris, R.C. (1997), *Spectral modelling of wind waves in coastal areas*, Ph.D.-thesis, Delft University of Technology, ISBN 90-407-1455-X, Delft University Press, Delft.

Ris, R.C., N. Booij, L.H. Holthuijsen, R. Padilla-Hernandez, IJ.G.Haagsma (1998), *Swan Cycle 2; User manual for version 30.75*, Delft University of Technology, Delft.

Roelvink, J.A. (1993), *Surfbeat and its effect on cross-shore profiles*, Ph.D.-thesis, Delft University of Technology, Delft.

Schäffer, H.A., R. Deigaard and P. Madsen (1992), *A two-dimensional surf-zone model based on the Boussinesq equations*, Proc. ICCE'92, Vol.1., pp.576-589, Venice.

Van Gent, M.R.A. (1994), *The modelling of wave action on and in coastal structures*, Coastal Engineering, Vol.22 (3-4), pp.311-339, Elsevier, Amsterdam.

Van Gent, M.R.A. (1995), *Wave interaction with permeable coastal structures*, Ph.D.-thesis, Delft University of Technology, ISBN 90-407-1182-8, Delft University Press, Delft.

Van Gent, M.R.A. (1999-a), *Wave run-up and wave overtopping for double peaked wave energy spectra*, Delft Hydraulics Report H3351-January 1999, Delft.

Van Gent, M.R.A. (1999-b), *Physical model investigations on coastal structures with shallow foreshores; 2D model test on the Petten Sea-defence*, Delft Hydraulics Report H3129-July 1999, Delft.

Tables

Foreshore: Spectral wave model

No.	SWL) (NAP)	H_{m0}			$T_{m-1,0}$			T_p		
		M	C	%	M	C	%	M	C	%
1.01	2.10	2.0	1.7	-14	9.6	7.6	-21	22.5	10.5	-53
1.02	2.04	1.9	1.6	-15	10.0	7.7	-23	17.9	10.9	-39
1.03	2.24	2.0	1.8	-8	10.0	8.5	-15	22.5	18.5	-18
1.04	1.66	1.7	1.6	-8	10.5	8.6	-18	22.5	18.2	-19
1.05	1.60	1.6	1.5	-8	9.9	7.7	-23	17.9	17.5	-2
1.06	2.04	1.9	1.7	-8	9.9	7.8	-21	19.2	14.3	-26
2.11	2.10	1.7	1.7	-2	7.1	6.0	-15	8.8	8.5	-3
2.13	2.10	2.0	1.5	-22	9.9	8.0	-19	14.8	12.2	-18
2.15	2.10	2.1	2.4	13	10.4	6.4	-39	16.7	15.2	-9
2.21	4.70	1.8	2.3	27	7.8	6.2	-21	8.6	8.3	-4
2.23	4.70	3.2	2.8	-12	9.0	8.5	-5	13.6	11.9	-13
2.25	4.70	3.7	3.7	1	10.7	7.6	-29	16.2	14.7	-9
2.31	2.10	2.0	1.9	-4	6.9	4.7	-32	6.9	7.2	4
2.41	4.70	2.9	3.4	15	6.7	4.8	-29	7.1	7.2	1
2.51	4.70	3.5	3.1	-11	7.9	6.8	-13	10.0	9.1	-9
2.54	4.70	3.6	3.5	-5	11.2	10.4	-7	18.5	18.2	-2
2.61	1.30	1.5	1.2	-24	10.3	7.8	-24	14.8	12.2	-18
2.71	2.10	1.9	1.5	-23	9.3	8.1	-14	22.5	12.2	-46
2.72	2.10	1.9	1.6	-16	9.5	7.6	-20	23.5	12.2	-48
2.73	2.10	1.9	1.6	-20	10.0	7.9	-21	22.5	10.5	-53

Table T2.1   Differences (in %) between measured (M) and computed (C) wave parameters at TOE (both based on wave energy spectra filtered between 0.04 and 0.3 Hz, based on 1000 waves).

Foreshore: Time-domain wave model											
No.	SWL)	H_{m0}			$T_{m-1,0}$			T_p		
	(NAP)	M	C	%	M	C	%	M	C	%
1.01	2.10	1.9	2.1	10	10.7	10.5	-1	16.4	15.4	-7
1.02	2.04	1.8	2.0	10	10.7	10.7	0	14.0	19.2	37
1.03	2.24	1.9	2.2	14	11.4	11.0	-4	17.1	18.4	8
1.04	1.66	1.6	1.9	15	11.9	11.0	-7	17.7	20.9	18
1.05	1.60	1.5	1.7	15	10.9	11.1	2	17.7	20.0	13
1.06	2.04	1.8	1.9	5	10.8	10.5	-2	18.4	16.4	-11
2.11	2.10	1.6	1.8	14	7.8	8.0	2	8.2	8.2	0
2.13	2.10	1.9	2.0	10	11.0	11.3	2	15.9	23.0	45
2.15	2.10	2.0	2.3	13	11.8	12.2	3	21.9	20.0	-9
2.21	4.70	1.8	2.2	24	8.0	7.6	-5	8.9	8.2	-7
2.23	4.70	3.1	3.3	4	9.4	10.1	8	13.2	12.1	-8
2.25	4.70	3.6	3.7	3	11.6	12.3	6	15.9	15.9	0
2.31	2.10	1.8	1.9	6	7.7	8.4	10	7.0	7.3	5
2.41	4.70	2.8	2.8	-1	7.1	7.2	1	6.9	6.9	0
2.51	4.70	3.3	3.1	-6	8.6	9.1	5	10.0	10.0	0
2.54	4.70	3.5	3.8	8	11.5	13.1	13	17.7	20.0	13
2.61	1.30	1.5	1.7	16	11.4	11.3	-1	16.4	19.2	17
2.71	2.10	1.8	1.9	5	10.4	10.7	3	18.4	11.0	-40
2.72	2.10	1.9	2.0	5	10.9	10.6	-3	17.1	20.9	23
2.73	2.10	1.9	2.0	8	11.1	10.4	-7	14.9	20.9	41

Table T3.1   Differences (in %) between measured (M) and computed (C) wave parameters at TOE (both based on wave energy spectra filtered between 0.04 and 0.3 Hz, based on 500 waves).

Structure: Wave run-up			
No.	$z_{2\%}$ (SWL)		
	measured	computed	difference %
1.01	4.7	4.2	10.5
1.02	4.8	4.8	0.2
1.03	5.3	4.7	11.4
1.04	5.3	4.7	10.5
1.05	4.1	3.8	9.3
1.06	4.7	4.5	4.1
2.11	< 3.6	3.0	
2.13	5.0	4.4	12.6
2.15	6.3	5.4	14.0
2.21	3.3	3.0	10.1
2.23	6.6	5.9	10.8
2.25	> 7.2	8.0	
2.31	< 3.6	3.1	
2.41	4.4	3.6	17.2
2.51	6.1	5.9	3.9
2.54	>7.2	8.3	
2.61	< 4.4	3.8	
2.71	5.0	4.2	15.2
2.72	5.1	4.8	6.3
2.73	5.1	4.7	8.9

Table T4.1   Comparison between measured and computed wave run-up levels (data-set with incident waves from measured surface elevations).

| Structure: Wave run-up			
No.	$z_{2\%}$ (SWL)		
	measured	computed	difference %
1.01	4.7	3.9	16.1
1.02	4.8	3.9	19.5
1.03	5.3	4.3	17.9
1.04	5.3	4.3	18.1
1.05	4.1	3.4	18.4
1.06	4.7	4.1	12.8
2.11	< 3.6	2.8	
2.13	5.0	3.8	24.4
2.15	6.3	4.3	32.1
2.21	3.3	3.3	1.5
2.23	6.6	5.8	11.8
2.25	> 7.2	7.6	
2.31	< 3.6	2.3	
2.41	4.4	3.5	19.2
2.51	6.1	5.1	17.4
2.54	>7.2	8.4	
2.61	< 4.4	3.1	
2.71	5.0	3.9	22.5
2.72	5.1	4.1	19.0
2.73	5.1	4.0	22.2

Table T4.2   Comparison between measured and computed wave run-up levels (data-set with incident waves from spectral foreshore model).

Structure: Wave run-up			
No.	$z_{2\%}$ (SWL)		
	measured	computed	difference %
1.01	4.7	5.0	-6.6
1.02	4.8	5.3	-10.0
1.03	5.3	5.2	1.5
1.04	5.3	5.0	4.9
1.05	4.1	4.1	9.1
1.06	4.7	4.4	6.4
2.11	< 3.6	3.3	
2.13	5.0	5.3	-5.9
2.15	6.3	6.4	-1.6
2.21	3.3	3.2	1.9
2.23	6.6	6.2	6.3
2.25	> 7.2	8.3	
2.31	< 3.6	3.9	
2.41	4.4	3.5	18.8
2.51	6.1	5.5	10.8
2.54	>7.2	8.4	
2.61	< 4.4	4.0	
2.71	5.0	4.5	9.2
2.72	5.1	5.3	-3.9
2.73	5.1	4.7	7.7

Table T4.3   Comparison between measured and computed wave run-up levels (data-set with incident waves from time-domain foreshore model).

Figures

.
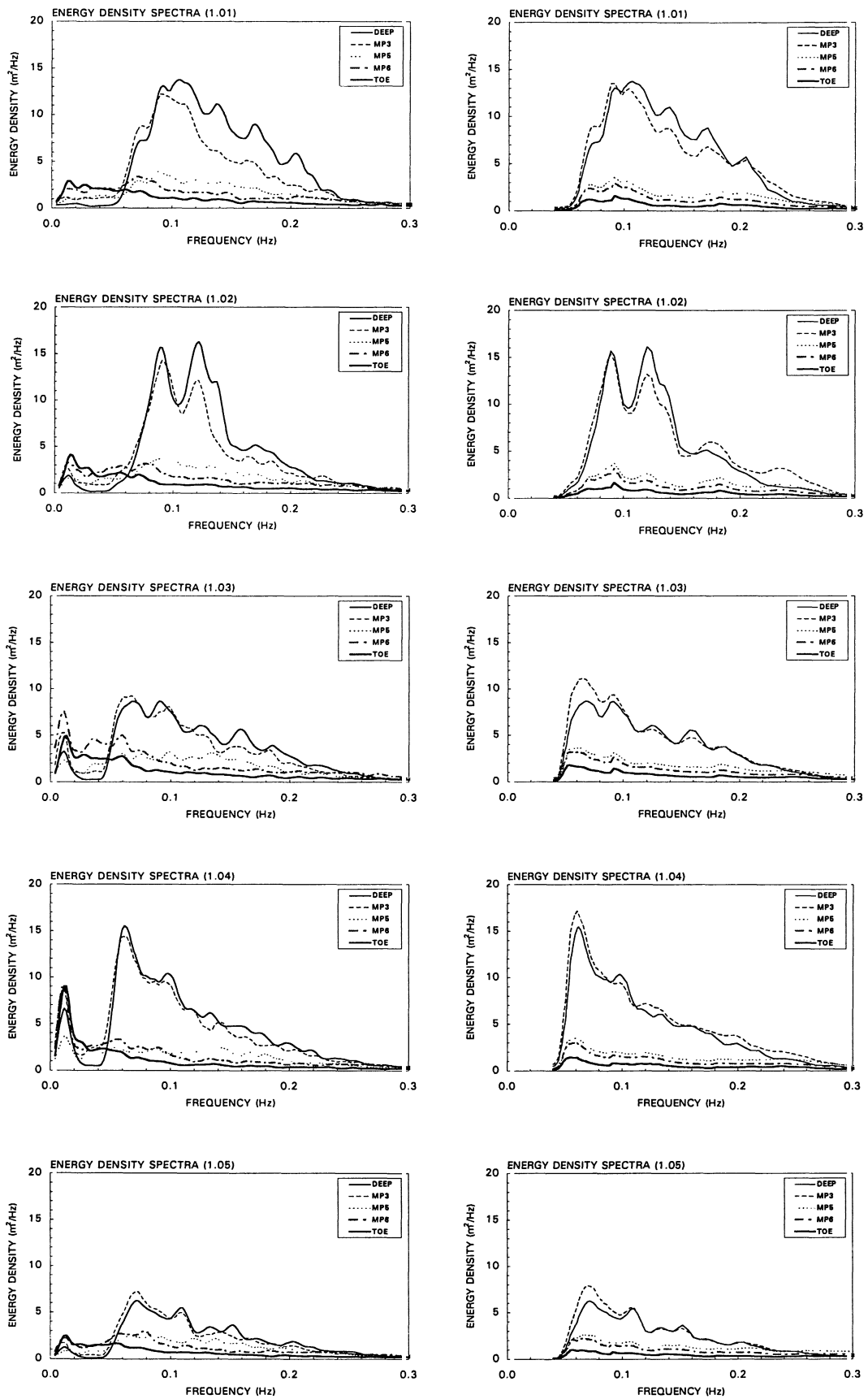
Figure F2.1a Comparison between measured (left) and computed (right) wave energy spectra, using the spectral wave model (Tests 1.01-1.05).
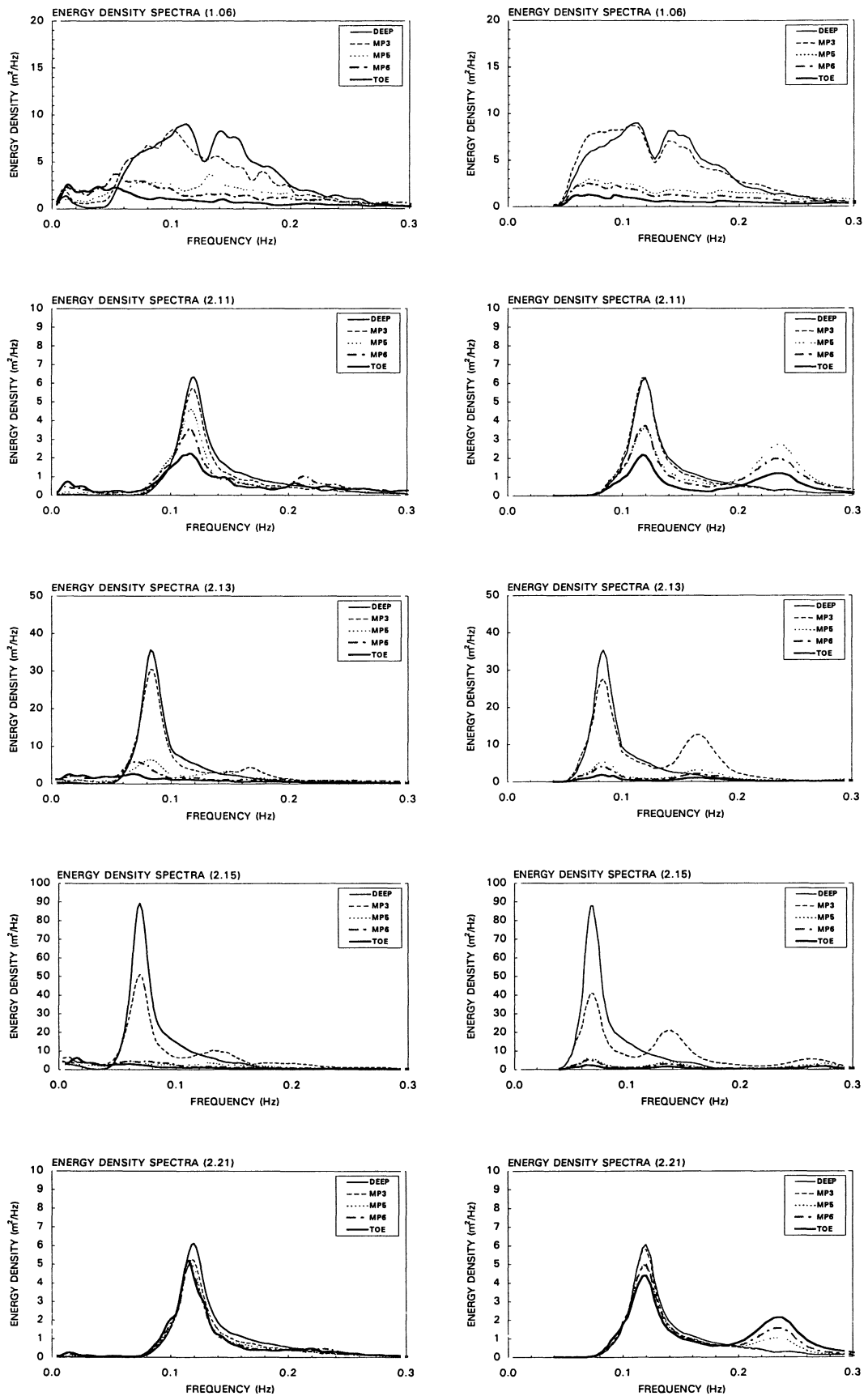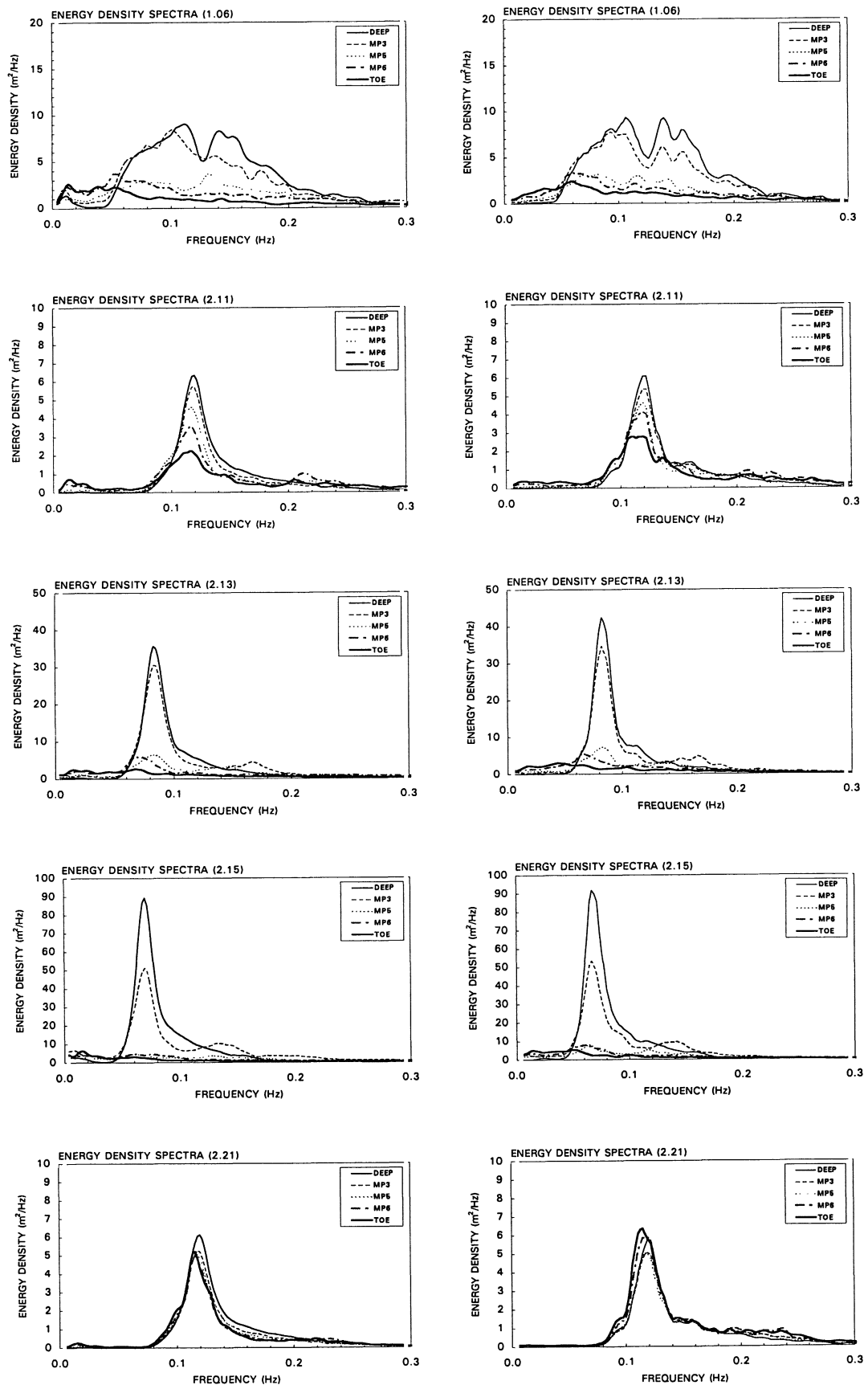
Figure F2.1b Comparison between measured (left) and computed (right) wave energy spectra, using the spectral wave model (Tests 1.06-2.21).
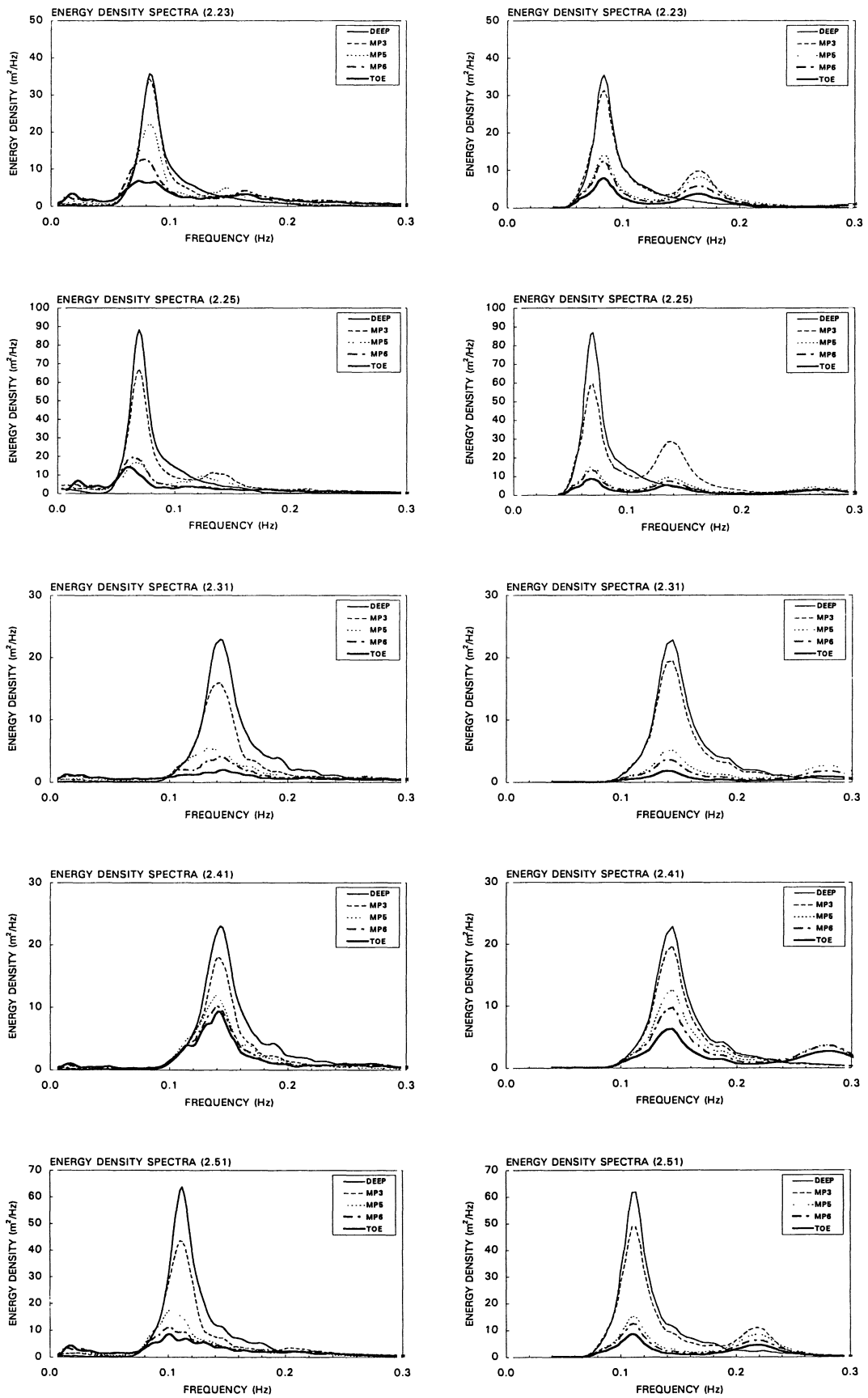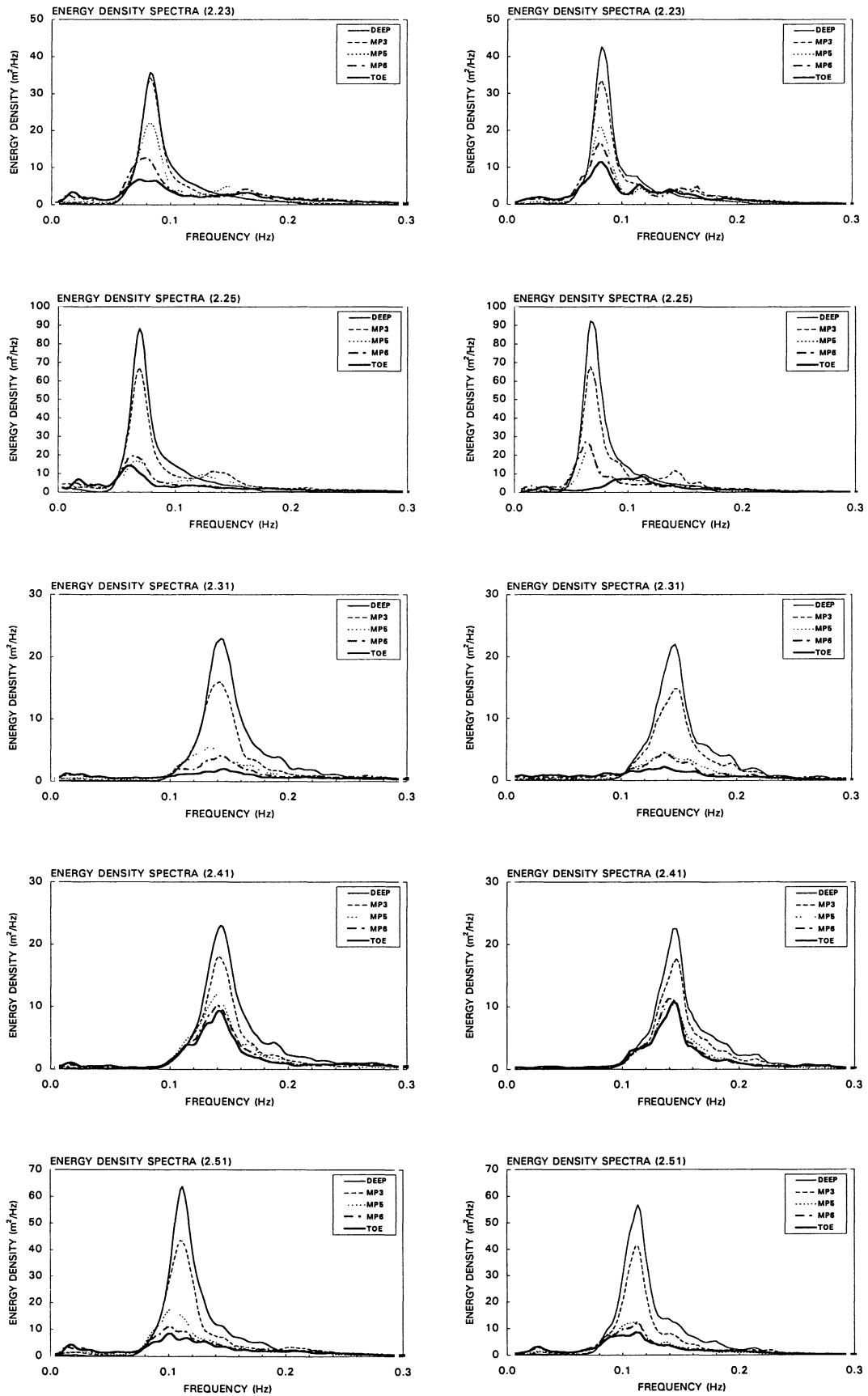
Figure F2.1c Comparison between measured (left) and computed (right) wave energy spectra, using the spectral wave model (Tests 2.23-2.51).
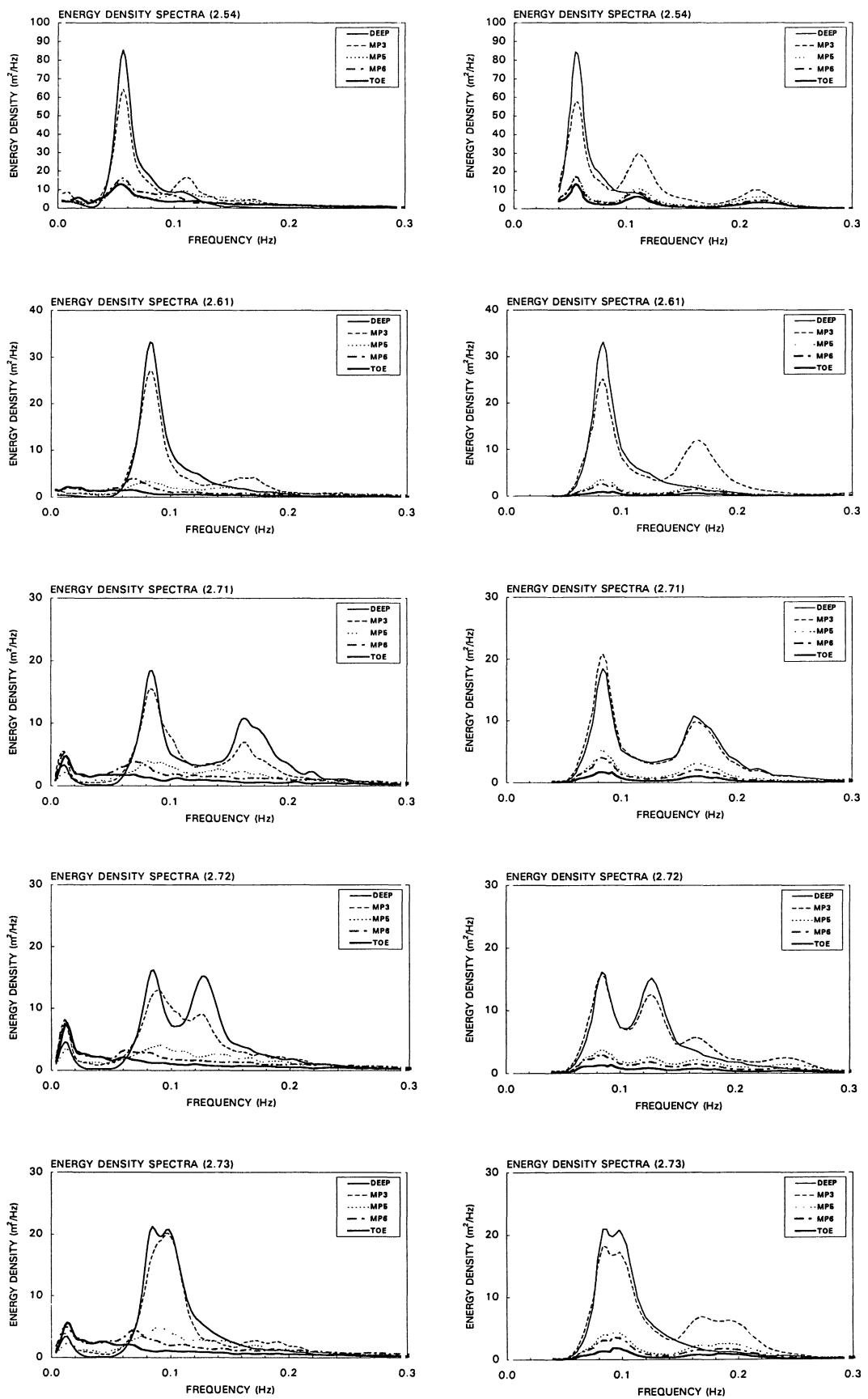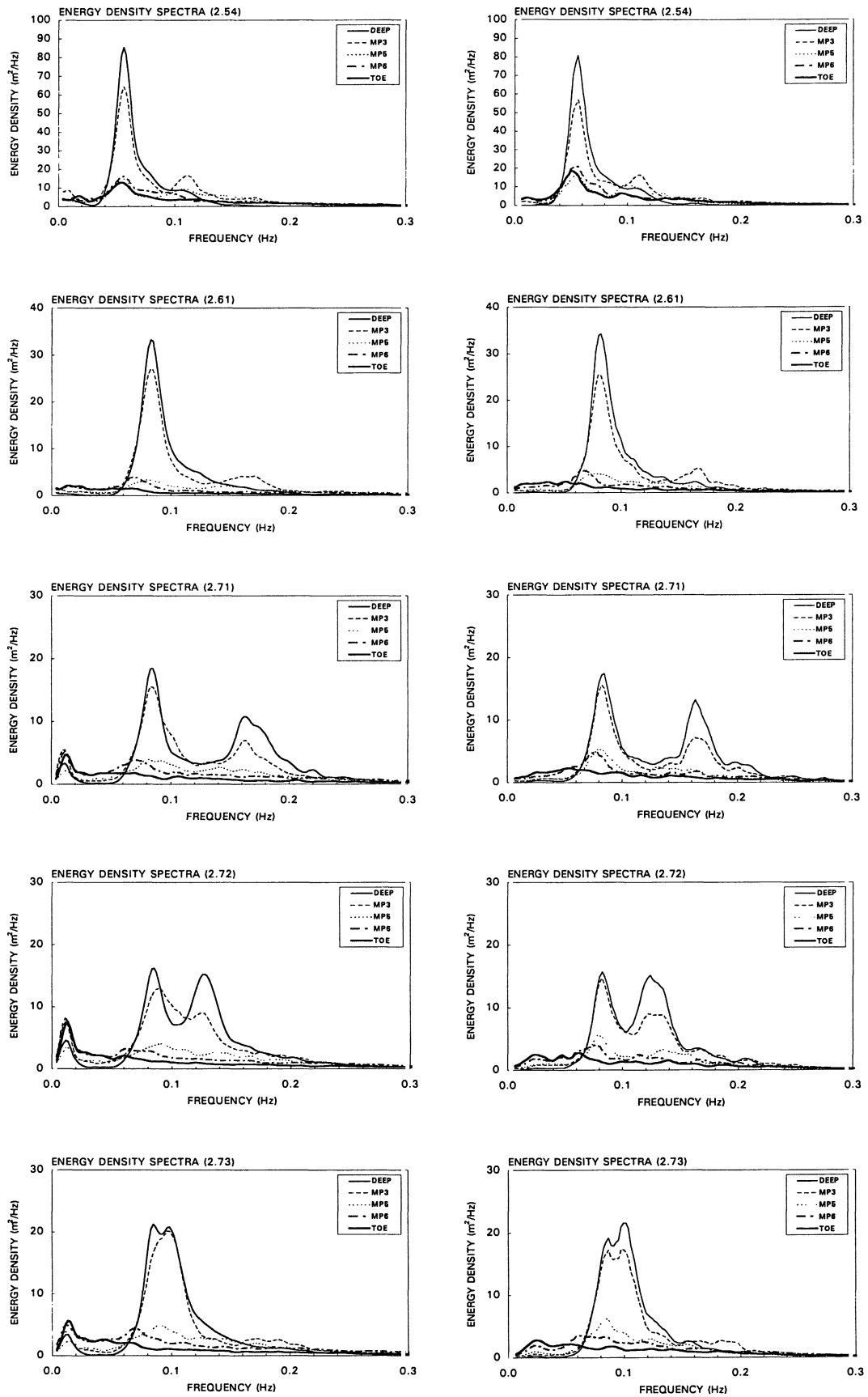
Figure F2.1d Comparison between measured (left) and computed (right) wave energy spectra, using the spectral wave model (Tests 2.54-2.73).
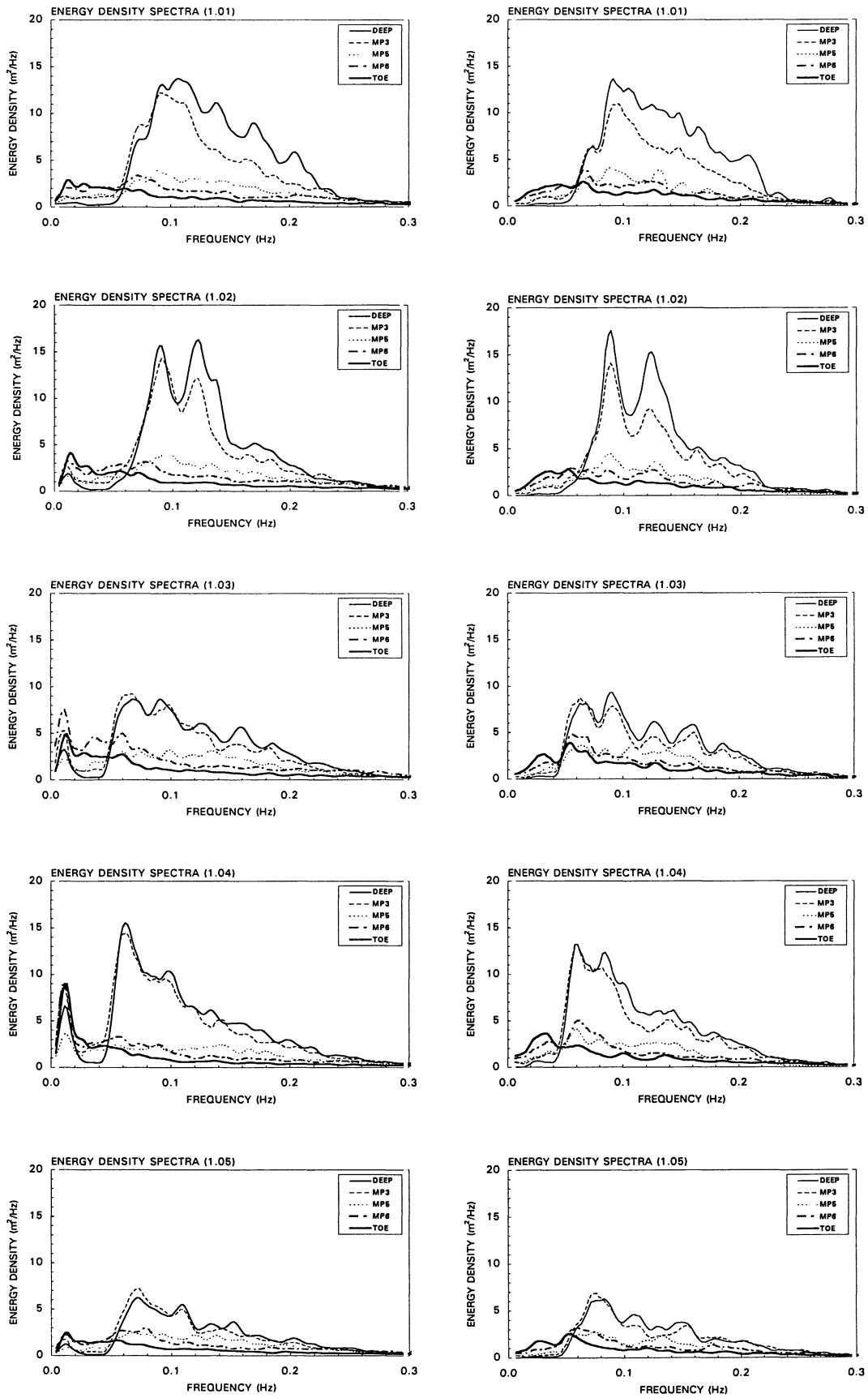
Figure F3.1a Comparison between measured (left) and computed (right) wave energy spectra, using the time-domain wave model (Tests 1.01-1.05).

Figure F3.1b Comparison between measured (left) and computed (right) wave energy spectra, using the time-domain wave model (Tests 1.06-2.21).

Figure F3.1c Comparison between measured (left) and computed (right) wave energy spectra, using the time-domain wave model (Tests 2.23-2.51).

Figure F3.1d Comparison between measured (left) and computed (right) wave energy spectra, using the time-domain wave model (Tests 2.54-2.73).
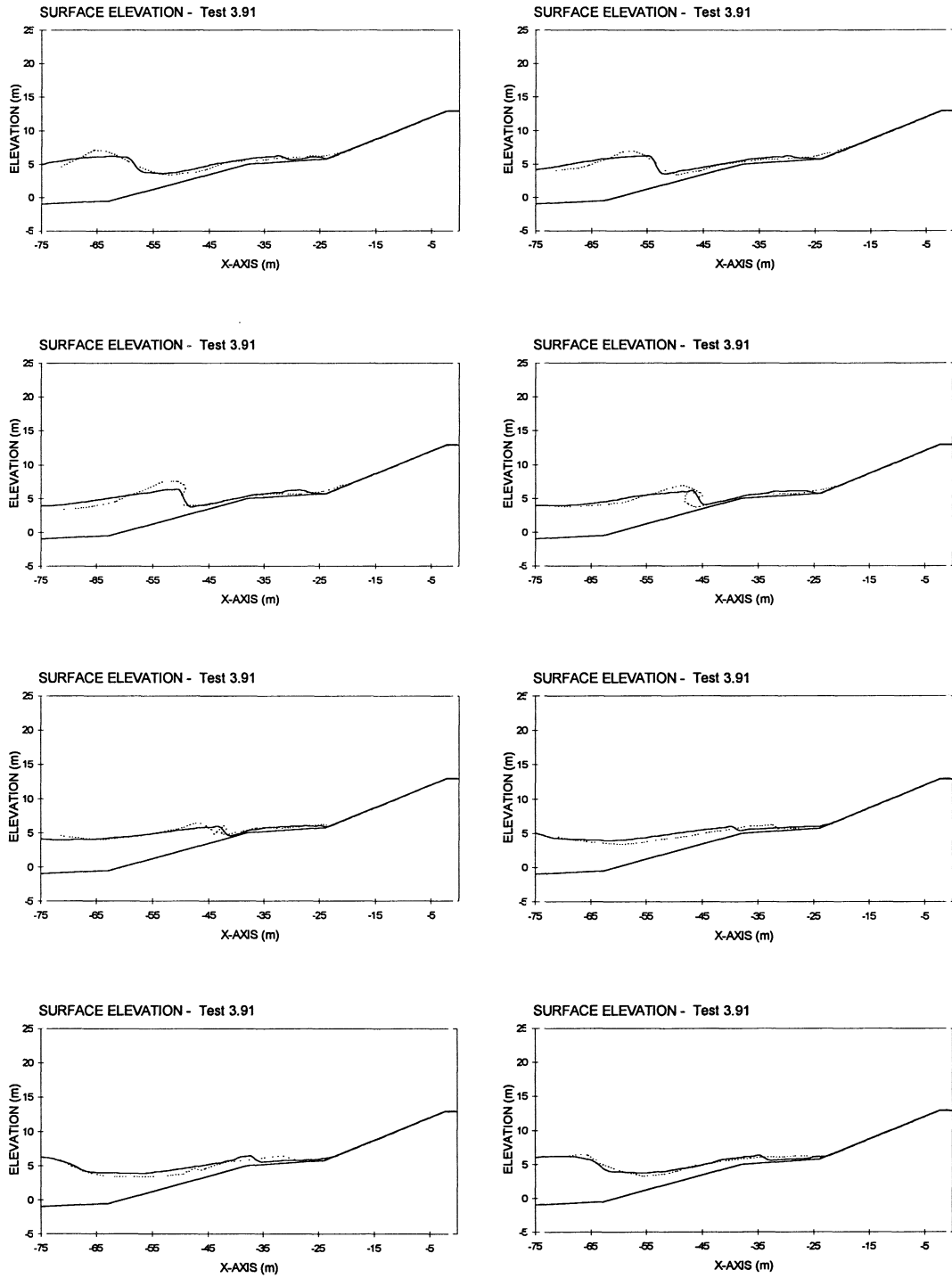
Figure F4.1   Measured (dashed) and computed surface elevations (Test 3.91), from Beck (1999).
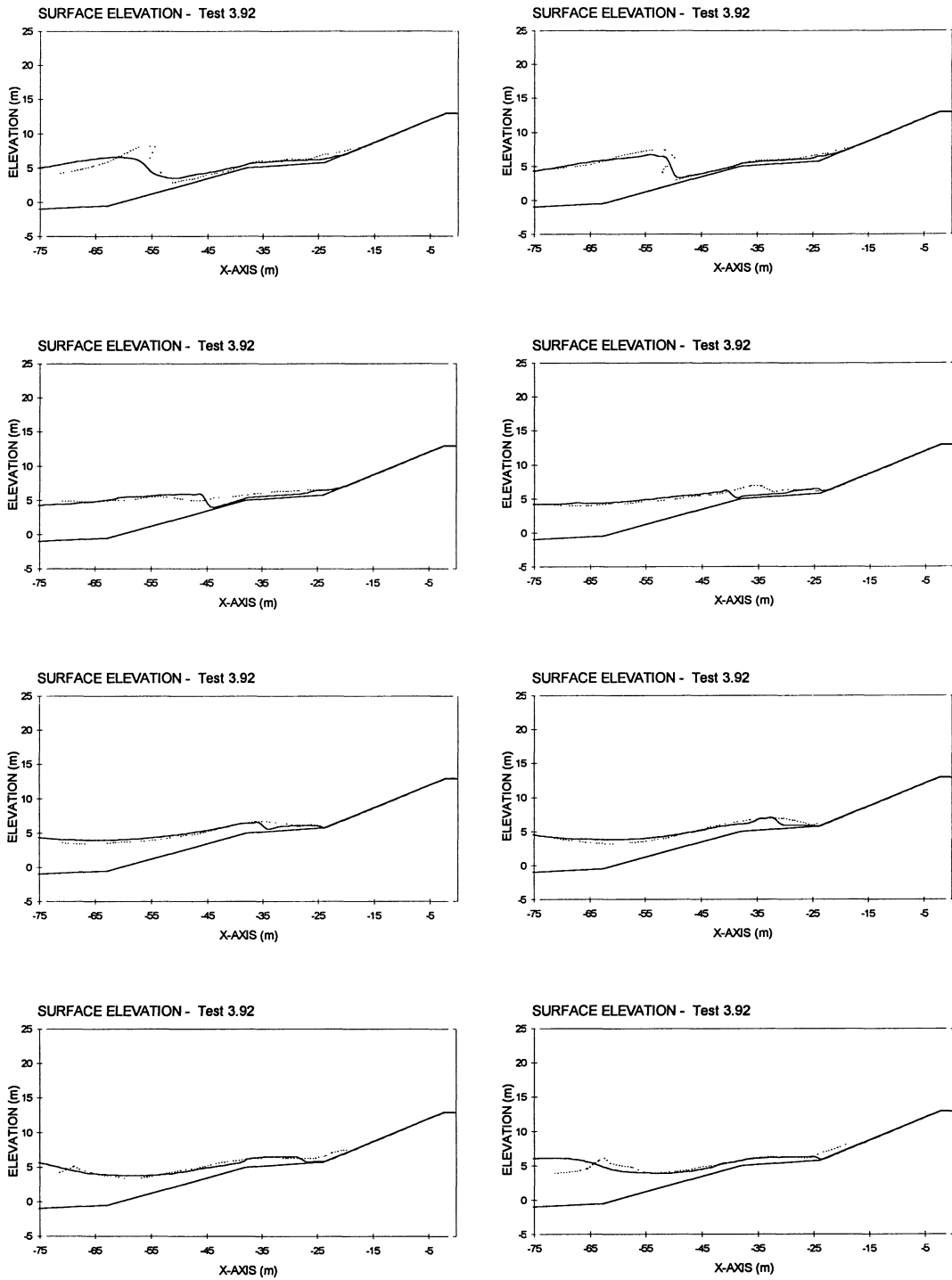
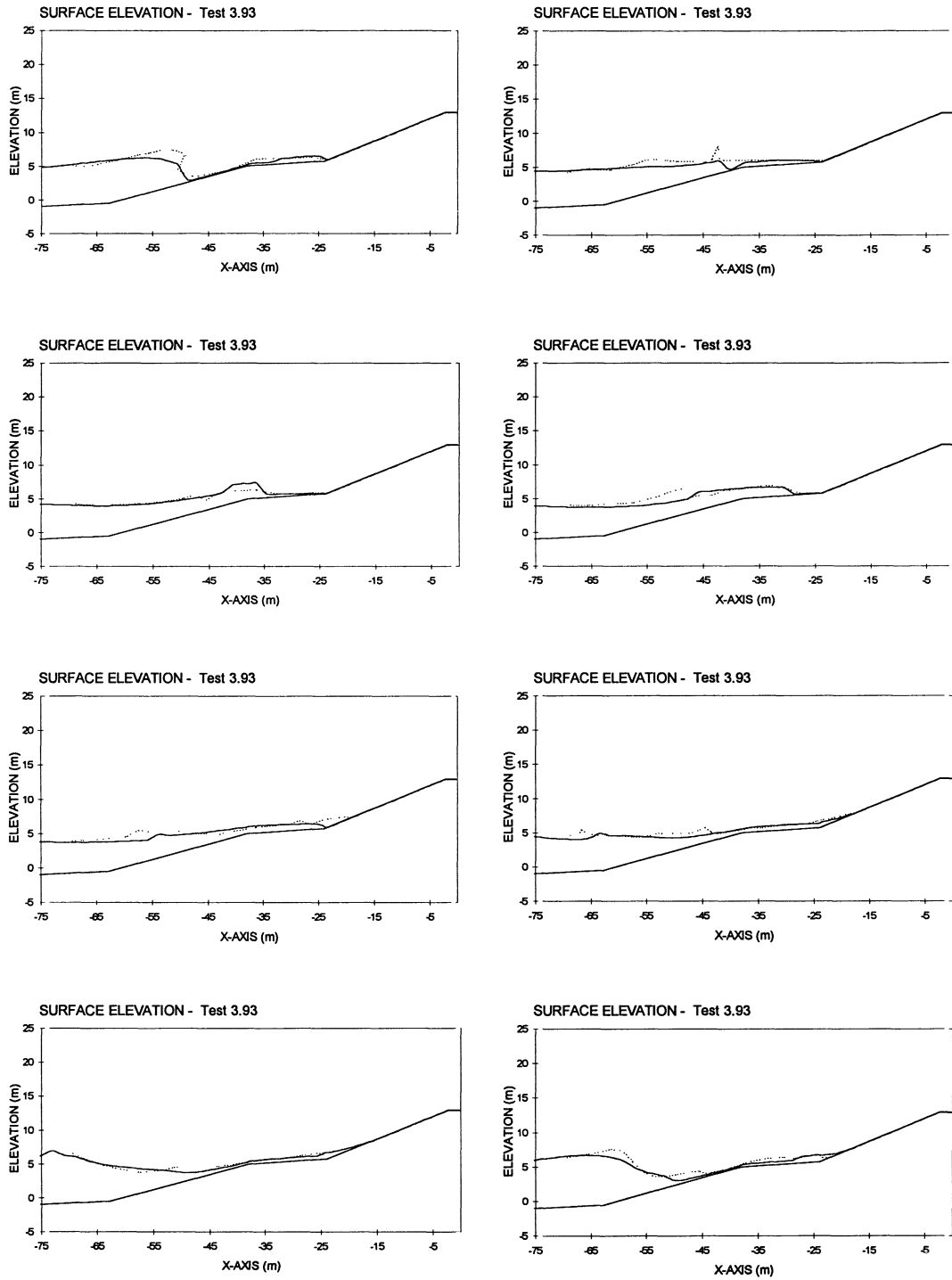Figure F4.2   Measured (dashed) and computed surface elevations (Test 3.92), from Beck (1999).

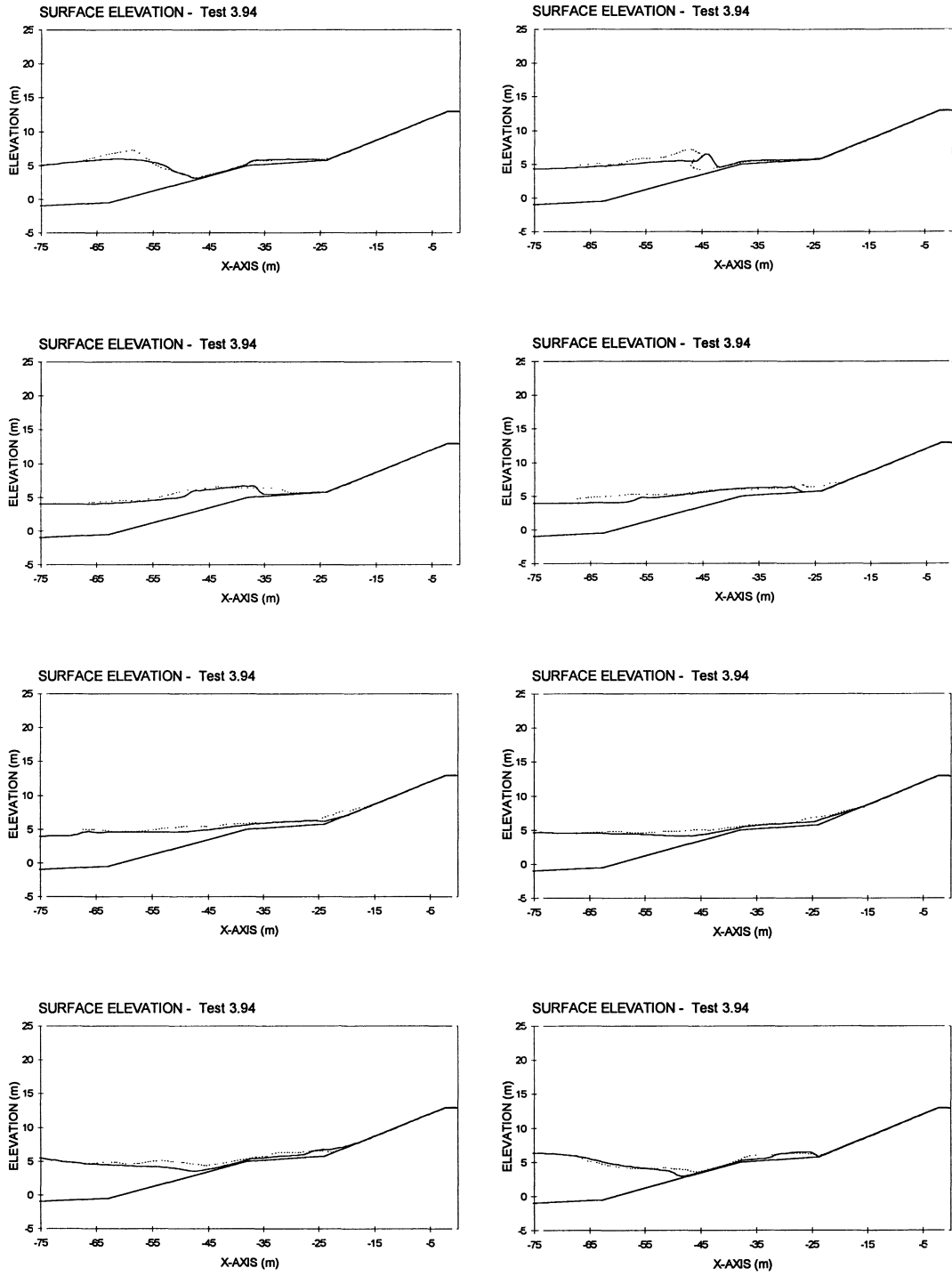Figure F4.3   Measured (dashed) and computed surface elevations (Test 3.93), from Beck (1999).

Figure F4.4   Measured (dashed) and computed surface elevations (Test 3.94), from Beck (1999).

WL | delft hydraulics

Delft

North Sea

Amsterdam

London